

# Supergen



Offshore  
Renewable  
Energy

## **Autumn Assembly 2022**

University of Oxford | 29 September 2022

# **Early Career Researcher Posters & Abstracts**



Engineering and  
Physical Sciences  
Research Council

# List of posters and abstracts

<b>01</b>	Dr Thomas Lake (Research Assistant, University of Swansea) - A Low-Cost, Modular, Open Source Datalogging System
<b>02</b>	Dr Hugo Putuhena (Research Fellow in Offshore Renewable Energy, University of Southampton) - Future scenarios for offshore wind (OW) in UK waters: spatial constraints, available space, and net zero targets
<b>03</b>	Dr Shen Li (Research Associate, University of Strathclyde) - Structural Analysis of Stinger Keel Floating Platform for Offshore Wind
<b>04</b>	Dr Kaushal Bhavsar (Postdoctoral Researcher, University of Hull) - Development of Fibre Optic Sensor System for monitoring unsteady loads on tidal turbine blade: Benchmarking Project
<b>05</b>	Euan Brough (PhD Student, University of Strathclyde) - Structural Damping Estimation of Wind Turbine Blades
<b>06</b>	Jade McMorland (PhD Student, University of Strathclyde) - Opportunistic maintenance for Scotwind Sites
<b>07</b>	Dr Xiaotao Zhang (PDRA, University of Manchester) - Modelling of a Wave Energy Converter Power Take-off, Considering Power Limiting Operation
<b>08</b>	Dr Bin Guo (Research Associate, Cardiff University) - The conjunctive operation of tidal range energy scheme on the west coast of the UK
<b>09</b>	Tom Tosdevin (COAST Researcher, University of Plymouth) - Short design waves for semi-sub FOWTs experiencing viscous drift
<b>10</b>	Aanantalakshmy Sihivahana Sarma (PhD Researcher, University of Hull) - Multi-Point Sensing of Wind Turbine Blade Loading for Structural Health Monitoring and Defect Detection
<b>11</b>	Karim Ali (PhD Student, University of Manchester) - Wind farm parameterisation in WRF
<b>12</b>	Laurence Morgan (PhD Candidate, University of Strathclyde) - Exploring the use of secondary rotors for vertical axis wind turbine power take off
<b>13</b>	Dr Tapas Kumar Das (Research Fellow, Queen's University Belfast) - Investigation into the Coupling of a Wave Energy Converter with a Reverse Osmosis Desalination Plant
<b>14</b>	Dr Sam Tucker Harvey (Postdoctoral Research Assistant, University of Oxford) and Dr Xiaosheng Chen (Research Assistant, University of Oxford) - Unsteady Loading Tidal Benchmarking Project
<b>15</b>	Markella Zormpa (PhD Student, University of Oxford) - Dynamic Mode Decomposition of Wind Turbine Wakes
<b>16</b>	Daniel Dehtyriov (DPhil Candidate, University of Oxford) - Flow Physics Beyond the Betz Limit
<b>17</b>	Dr Jamie Crispin (Postdoctoral Research Assistant, University of Oxford) - Implementing HARM in a 1D Winkler model to predict monopile response to cyclic loading
<b>18</b>	Dr Razieh Jalal Abadi (Research Fellow, University College London) - Surface Waves in Open-Channel Flow Over Spanwise Aligned Square Bars
<b>19</b>	Morgane Declerk (PhD Student, University of Aberdeen) - A new strategic tool to structure Cumulative Impact Assessment (CIA)
<b>20</b>	Dr Miad Saberi (Postdoctoral Researcher, University of Oxford) - Three-Dimensional Finite Element Modelling of Laterally Loaded Monopiles in Sand
<b>21</b>	Jingyi Yang (DPhil Candidate, University of Oxford) - Origami inspired clam type wave energy converter

## Overview

Following on from work on the SURFTEC project, this part of the Selkie project is looking at the use of a low-cost datalogger based around a single-board computer and a modular software platform.

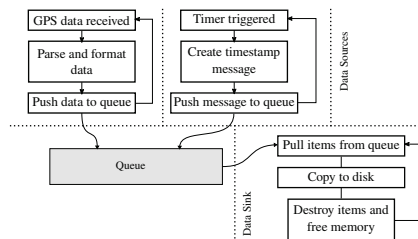
Requirements identified as part of the previous project or its review included:

- designed to operate from low voltage DC
- able to record multiple serial data streams
- able to timestamp recorded data
- flexible enough to allow use with different combinations of sensors and equipment

The system uses a Raspberry Pi 4, interfacing with other sensors using a combination of directly connected hardware, serial/USB links, and network communication.

The Pi itself has no analog inputs, so these are provided by an expansion board connected to the Pi and dedicated ADC adaptors connected to an Arduino, which provides the data to the Pi over a USB serial connection

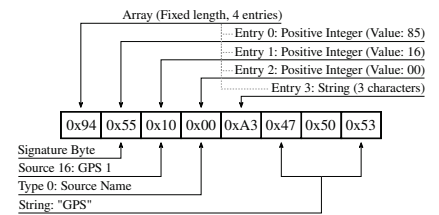
## Data Flow



The core of the logging software is implemented in C. Each data handler runs in its own thread, reading in data and converting it into suitably formatted messages. These messages are then queued before another thread removes messages from the queue and writes them to disk.

The messages contain no timing information, so timestamp messages are generated at a fixed rate and added to the queue. The interval between these timestamps defines the temporal resolution of output data - a particular message (for example, representing a sensor reading) is only known to have been pushed at some point after the preceding timestamp and before the next one.

## Message Structure



A common message format has been defined for the project, and all incoming data is converted or encapsulated in these messages for storage and further processing.

The msgpack standard is used to encode the data, with each logged message consisting of 4 parts as shown above:

- A signature or marker byte
  - Source ID
  - Message type
  - Message data
- The format allows up to 127 simultaneous data sources  
Up to 127 types can be defined, although 6 are predefined.
- This can be one or more strings or floating point values

## Supported Data Sources

The software currently supports the following sources:

- u-Blox GPS receivers
- NMEA message sources
  - GPS position, velocity and time data
  - Environmental data
- I<sup>2</sup>C devices
  - Analog to digital converters (ADCs)
  - Support is chip specific, but includes voltage and current measurements
- Datawell Waverider HXV messages
- MQTT data

Additionally, any network (TCP) or serial stream can be captured and recorded for later extraction, even if the values aren't interpreted in real time. This allows data for one day to be collected in a single file, for later extraction and analysis using standard tools.

## Testing



Principal testing has been carried out in conjunction with MEECE and ORE Catapult on a measurement buoy deployed at Dale Roads, just outside Milford Haven in south west Wales.

This test deployment includes a Waverider, multiple analog sensors, an interface with the buoy's on board power management system and the GPS and marine (NMEA) instruments on board.

## Related other work

A separate part of the Selkie project has been the design, development, and testing of a converging beam ADP device at the Marine Energy Test Area (META) in Milford Haven.

The core hardware is similar but lacks the internet connection present on the MEECE buoy. This allowed the testing of dedicated real time clock hardware and power reduction, which may be useful for future logging system deployments.



The financial support of the Selkie Project is acknowledged.  
The Selkie Project is funded by the European Regional Development Fund through the Ireland Wales Cooperation programme.

# A Low-Cost, Modular, Open Source Datalogging System

T. Lake<sup>1</sup>, I. Masters, A. J. Williams

Energy and Environment Research Group, Faculty of Science and Engineering,  
Swansea University

<sup>1</sup>t.lake@swansea.ac.uk

**KEYWORDS:** data logging, instrumentation, field measurements

Previous work on the SURFTEC project led to the design and deployment of a remotely accessible data recording system based around a combination of a commercially available automotive data logger and a low cost single-board computer[1]. This combination allowed the system to be developed around a small amount of bespoke software and offloaded the bulk of the data recording to a proven off the shelf device. The use of a commercial system did impose some limitations on the type of data able to be recorded, and some instruments were recorded separately in parallel on the control PC[1], [2].

In order to overcome some of these limitations, development of a software based logging solution has been taking place under the SELKIE project. This provides a flexible platform to record data from analog and digital sources, including data from serial or network connected devices such as GPS receivers, NMEA devices, and other common instruments.

The system takes a modular approach, with each software or hardware component using a common message format to communicate values between them. Each data source is configured in software such that data is read from hardware (or generated in situ) before being placed in a common queue. Messages are then taken from the queue and copied to disk.

Testing of the system is being carried out in conjunction with ORE Catapult, with information from GPS receivers, a range of marine instruments and a Datowell waverider being recorded and uploaded to cloud storage on a daily basis for analysis on shore.

Some hardware components have also been tested on the SELKIE converging beam ADCP device and a lab test rig as part of the MEECE project, demonstrating operation in an offline context and the ability to interface with other control systems.

- [1] T. Lake, A. J. Williams, and I. Masters, 'Ups and Downs of Data Recording on Tidal Devices', in *Proceedings of the 14th European Wave and Tidal Energy Conference*, Plymouth, UK, Sep. 2021, pp. 1888–1-- 1888–7.
- [2] T. Lake *et al.*, 'Strain gauge measurements on a full scale tidal turbine blade', *Renewable Energy*, vol. 170, pp. 985–996, Jun. 2021, doi: 10.1016/j.renene.2021.01.137.

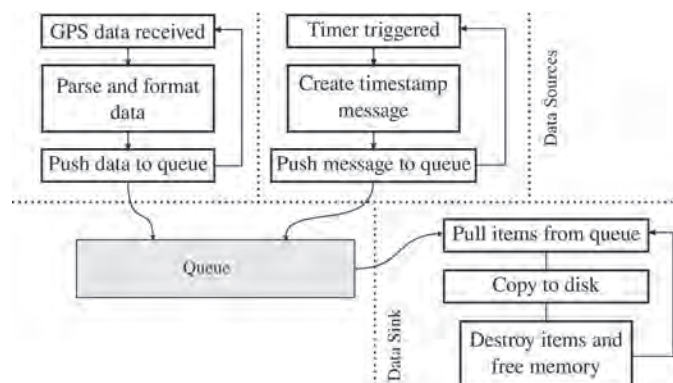


Figure 1: General software structure, with multiple data sources feeding information to a central queue to be recorded to storage.

# Future scenarios for offshore wind (OW) in UK waters: spatial constraints, availability space, and net zero targets

H Putuhena<sup>1\*</sup>, D White<sup>1</sup>, S Gourvenec<sup>1</sup>, F Sturt<sup>2</sup>

1 – Civil, Maritime and Environmental Eng., Uni of Southampton, UK, 2 – Archaeology, Uni of Southampton, UK  
 \* - Corresponding Author: [h.s.putuhena@southampton.ac.uk](mailto:h.s.putuhena@southampton.ac.uk), Website: <https://www.southampton.ac.uk/iroe>

## Outlines

- Demands of OW energy to meet the needs of net zero targets in energy transition sector by 2050 are keep growing: see Fig.1 for the approximation of the range of the total area needed from the growing demands of OW needed to fulfil electricity generation/green hydrogen/energy export by 2050.
- There is a need to balance the net zero targets with environmental impact to meet a sustainable blue economy.
- **Q:** How to define that balance into the spatial analysis in future sites selection?
- This study provides a new approach in spatial analysis to address the critical question: the quantification of the congestion level of spatial constraints that based on a collection of public dataset and observation of current leased sites, see Fig.2 and results in Fig.3.
- **Outputs:** future scenarios for future OW in the UK-EEZ waters based on the new approach spatial analysis, see Fig.4-5 & interactive dashboards.

## Future OW demands

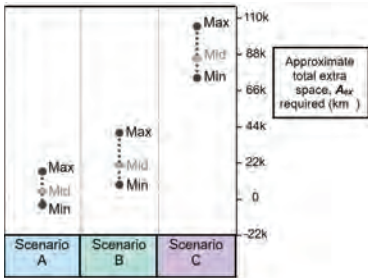


Fig.1: Future OW demands figured by the approximation of total extra space,  $A_{ex}$ , required from different scenarios of net zero targets: [A] electricity generation only, [B] electricity generation + green hydrogen, and [C] electricity generation + green hydrogen + energy export.

## Spatial analysis: New approach

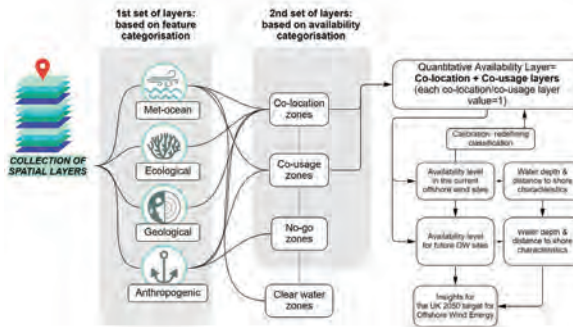


Fig.2: The flowchart of the new approach of spatial analysis method conducted in this study.

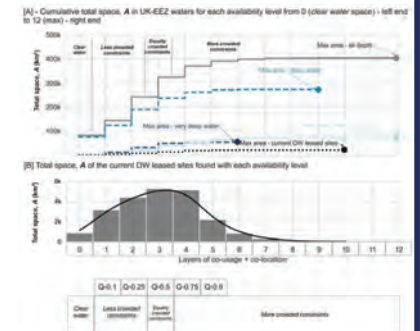


Fig.3: Availability level in the UK-EEZ waters and the classification based on the current OW leased sites data.

## Spatial analysis: Future scenarios

### Future Scenario 1:

(i) up to less crowded, (ii) shallow-deep water, and (iii) <197 km dist. to shore

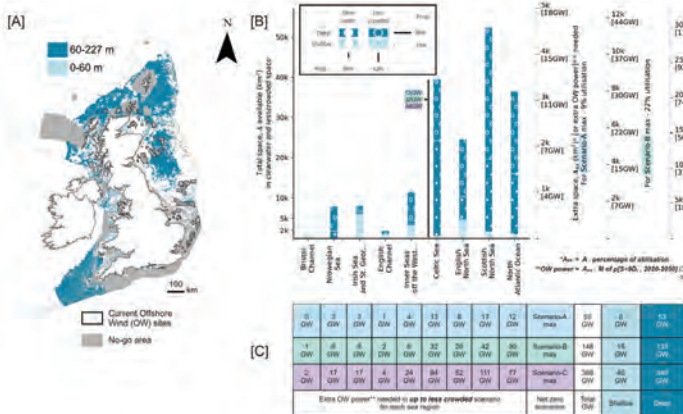


Fig.4: Future scenario 1 in [A] Total available space A in map, [B] bar charts of A (left-axis) with required extra space  $A_{ex}$  (right-axis) for different scenarios A-C, and [C] Table of extra OW power needed for each water range and net zero scenarios.

### Future Scenario 2:

(i) up to equally crowded, (ii) shallow-deep water, and (iii) <197 km dist. to shore

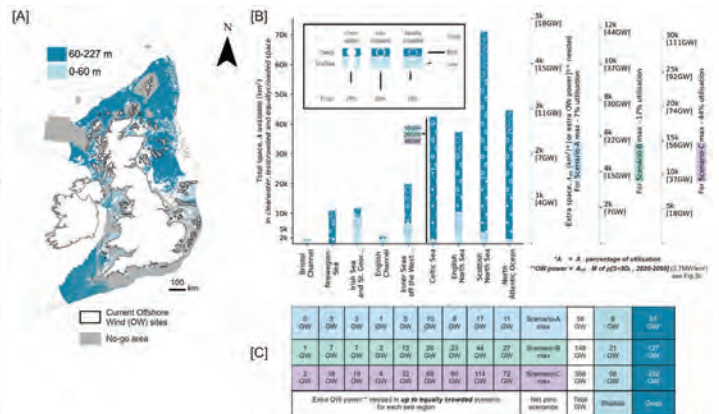


Fig.5: Future scenario 2 in [A] Total available space A in map, [B] bar charts of A (left-axis) with required extra space  $A_{ex}$  (right-axis) for different scenarios A-C, and [C] Table of extra OW power needed for each water range and net zero scenarios.

## Insights for net zero OW targets

Results above show the urgent need of:

- elimination of the water depth barrier through floating OW technology
- opening up of new sea regions and the associated port and grid infrastructure
- assessment of the potential impact of increased utilisation of ocean space for OW

## Further look: Interactive Dashboards



## Acknowledgments

This project is funded by Supergen Offshore Renewable Energy (ORE) Hub (EPSRC grant ref.EP/S000747/1), the RAEng Centre of Excellence in Intelligent & Resilient Ocean Engineering (IROE) and Southampton Marine and Maritime Institute (SMMI).

**POSTER TITLE for SUPERGEN ORE HUB, ECR Autumn assembly:**

‘Future scenarios for offshore wind (OW) in UK waters: spatial constraints, available space, and net zero targets’

**ABSTRACT**

Hugo Putuhena<sup>1\*</sup>, David White<sup>1</sup>, Susan Gourvenec<sup>1</sup>, Fraser Sturt<sup>2</sup>

1 – Civil, Maritime and Environmental Eng., Uni of Southampton, UK

2 – Archaeology, Uni of Southampton, UK

\*h.s.putuhena@southampton.ac.uk

**ABSTRACT**

This study estimates that between ~22k-110k km<sup>2</sup> extra space will be required for offshore wind (OW) if net zero targets are to be met by 2050. The extent of this area varies depending on if the demand is solely for UK electricity generation or is enhanced by needs for green hydrogen and energy export. These targets need to be met within spatial and environmental constraints. This study presents a new approach to spatial analysis that supplies a quantification of the UK waters’ congestion level of spatial constraints as a tool support this planning. Two different scenarios for OW were derived from a quantitative layer. The first scenario involves OW developments only in areas that are less constrained than locations currently licensed and in use. The second scenario extends to sea regions that are *equally crowded* as the current OW leased sites. The geospatial models from both scenarios show that after constrained zones are eliminated, up to around half of the remaining available UK sea area needs to be used for future OW. These results highlight the importance of technological advances for floating wind to minimise the barrier to OW development in deep water depth, the need to open up new UK sea region to OW development, and the need for continuity assessment in the environmental impact for future sites.

# Structural Analysis of Stinger Keel Floating Platform for Offshore Wind

Shen Li, Baran Yeter, Maurizio Collu, Feargal Brennan  
University of Strathclyde, Glasgow, UK

Gary Ross  
Floating Energy System Ltd, Surrey, UK

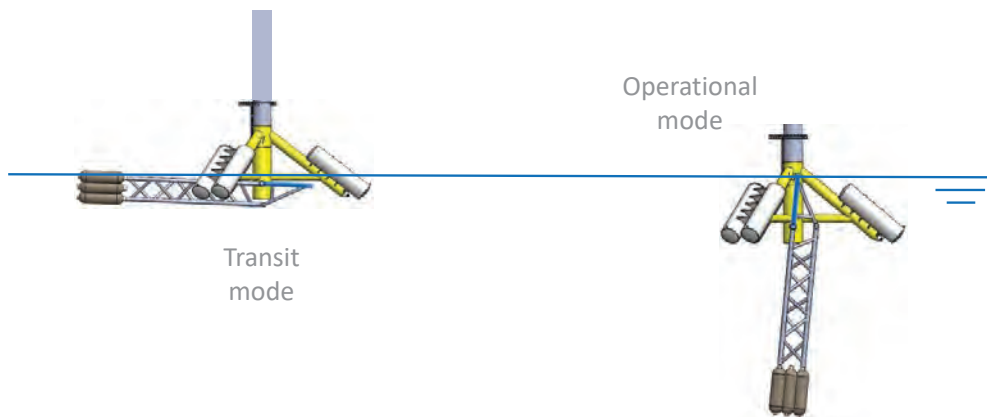


Figure 1. A hybrid spar/semi-submersible Stinger Keel Concept

## Stinger Keel Concept

The Stinger Keel is a novel floating offshore wind turbine foundation design. It is a spar-based structures assembled, launched and towed as a semi-submersible. It has the benefits of a spar-type foundation (e.g., reduced hydrodynamic motion) for deep water operation but, unlike the conventional spars, can be built in the quayside (shallow water).

## Research Objectives

- Strength analysis – verifying the adequacy of structural scantling in various environment conditions based on an ultimate limit state criterion.
- Integrity analysis – assessing the durability of critical structural detail in the most typical operational mode based on an fatigue limit state criterion.

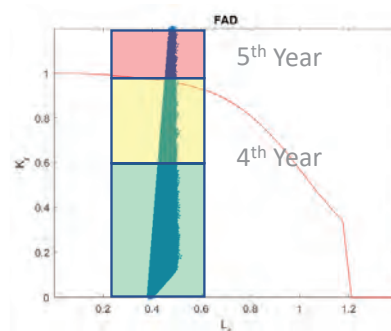
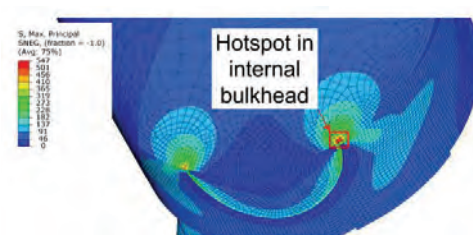
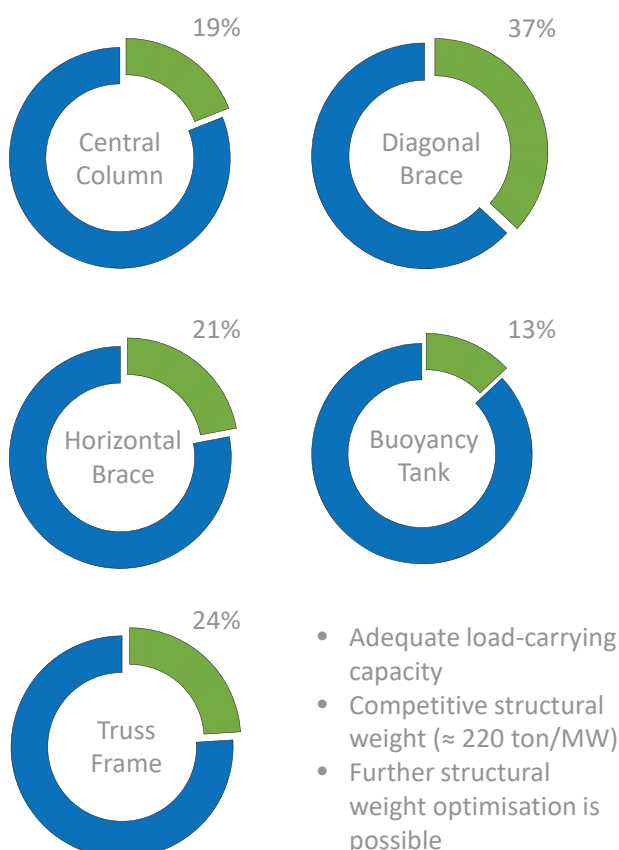


Figure 3. Failure assessment diagram

## **Structural Analysis of Stinger Keel Floating Platform for Offshore Wind**

Shen Li

The Stinger Keel is a novel floating offshore wind turbine foundation design. It is a spar-based structures assembled, launched and towed as a semi-submersible. It has the benefits of a spar-type foundation (e.g., reduced hydrodynamic motion) for deep water operation but, unlike the conventional spars, can be built in the quayside (shallow water). In this project, the University of Strathclyde collaborates with a multidisciplinary consortium led by Floating Energy System to perform structural analysis for the Stinger Keel foundation structures in the light of verifying its structural adequacy and optimising the structural design. Two types of structural analysis criteria are considered: Ultimate Limit State (ULS) and Fatigue Limit State (FLS). The former concerns with the maximum load-carrying capacity of the structures in extreme conditions, while the latter evaluates the durability of local structural details under repeated loading. A series of Finite Element Analyses (FEA) are performed on the Stinger Keel sub-structures under typical operational modes from normal to extreme environmental conditions. The ULS assessment is performed with a working stress principle, i.e., comparing the FEA-based working stress with codified criteria. The FLS evaluation is performed via SN curve and linear elastic fracture mechanics approach, in which the crack growth assessment and failure assessment diagram are conducted. The analyses demonstrate that the Stinger Keel sub-structures is a verified design with adequate maximum load-carrying capacity and competitive structure weight with respect to other floating offshore structure design. In terms of the fatigue performance of critical structural detail, regular inspections are needed after three years in operation. Alternatively, a structural health monitoring system can be introduced to ensure the structural integrity.

# Development of Fibre Optic Sensor System for Monitoring Unsteady Loads on Tidal Turbine Blade: Benchmarking Project

Dr Kaushal Bhavsar<sup>1</sup>, Miss Aananthya Sarma<sup>1</sup>, Dr Sam Tucker Harvey<sup>2</sup>, Dr Thomas Allsop<sup>1</sup>, Prof James Gilbert<sup>1</sup>, Prof Richard Willden<sup>2</sup>

<sup>1</sup>Faculty of Science and Engineering, University of Hull  
<sup>2</sup>Department of Engineering Science, University of Oxford

## Abstract

Fibre optic sensors offer many advantages when it comes to measurement in harsh environmental conditions due to its small size, immunity to electromagnetic interference, multiplexing capability and chemical inertness. This poster presents the design and development of the fibre optic sensor system for monitoring unsteady loads on the tidal turbine blade for the benchmarking project. For details about benchmarking project please refer to: <https://supergen-ore.net/projects/tidal-turbine-benchmarking>

## Introduction

Fibre optic sensors are widely used in many structural health monitoring applications including condition monitoring of wind turbine blades. Measuring the strain is one of the most effective methods to monitor blade loading conditions. A specific type of fibre optic sensor, called Fibre Bragg Gratings (FBG), are used for measuring the strain at given discrete locations on the turbine blade.

## Strain measurement

An optical fibre with Fibre Bragg gratings sensor is illustrated in fig 1. When broadband light is launched into the fibre, FBGs reflect the part of the spectrum at the designed wavelength. The rest of the spectrum is transmitted as seen in the transmitted spectrum. When an external longitudinal force is applied to the sensor, it causes a change in the sensor's physical properties and results in a shift in the designed peak position of the sensor. This shift in the peak position directly relates to the applied force. Strain resulting from the applied force on the sensor can be measured as illustrated in the schematic by monitoring the reflected peak position.

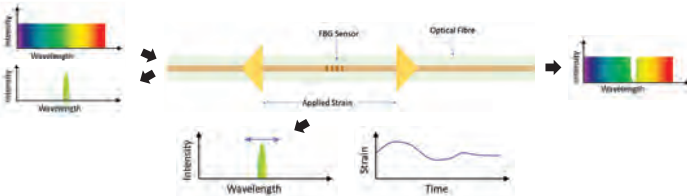


Figure 1 Schematic illustration of strain measurement using FBG sensor

## Fibre Optic Sensor System Design

The developed tidal turbine for the benchmarking study project has 3 bladed rotor of 1.6m diameter. The diameter of the nosecone is 0.2m in which the Fibre optic sensor (FOS) system is integrated. Considering the space constraints within the turbine design for the instrumentation, a system is designed with three small and portable instruments i.e. light source, an interrogator and a 1x4 optical switch. Fig 2(a) shows the schematic diagram of the FOS system. All the instruments are mounted within the nosecone as shown in the cad diagram in fig 2(b). The electrical interface to the instruments for power, control and data acquisition runs through the slip ring.

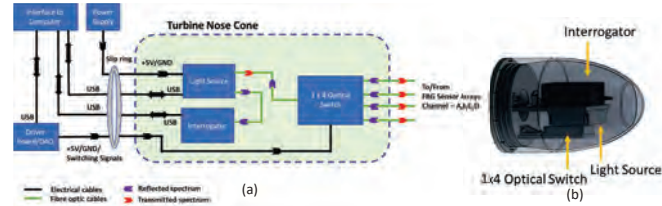


Figure 2 (a) Schematic of the fibre optic sensor system and (b) a cad diagram of the system integrated within nosecone

Figure 3(a) shows the schematic diagram of the placement of FBG sensors within a slot designed to install 24 strain sensors at six discrete radial locations (as shown in fig 3(b)) across the blade length. Four fibre optic sensor arrays are used with six sensors in each for strain measurement and are installed close to the corners of the slot to measure flapwise and edgewise loads, as shown in Fig 3(c). Also, there are two temperature sensors installed to compensate for any temperature variation during the test.

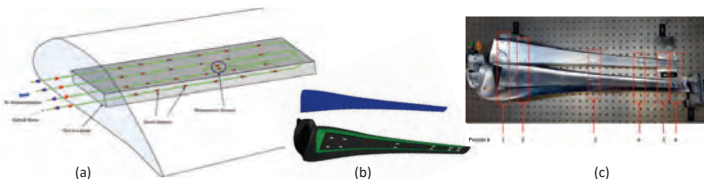


Figure 3(a) Schematic illustrating the installation of 26 FBG sensors within a slot. (b) Cad diagram of the blade showing the sensor locations and (c) picture of the turbine blade with installed sensors at six locations along the blade length.

## Results and discussions

Spectrum collected from channel 1 is shown in fig 4(a) which has six FBG strain sensors installed inside the blade slot as mentioned earlier. The dots on the peaks are the data points corresponding to system resolution of 0.17nm. Fig 4(b) shows the peak positions monitored over the time under no load conditions.

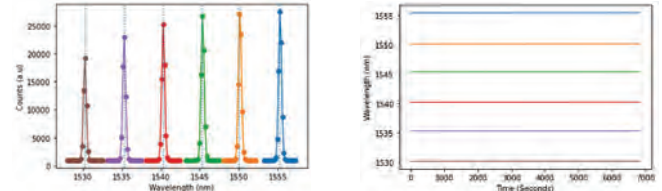


Figure 4(a) Channel 1 spectrum of the six FBG strain sensors and (b) their corresponding peak positions monitored over time under no load condition.

Figure below shows how the strain profile changes across the blade when a tip load is applied to the blade in flapwise direction as illustrated in fig 5(a). Data values on the plots are not revealed because data is yet to be released. Fig 5(b) shows the measured strain when load is increased in uniform steps. All the six FBG sensors have shown linear response to the applied load for a given loading scenario while experiencing different strain at respective discrete locations. Effect of loading at sensor positions across the blade is shown in fig 5(c) and (d) for positive and negative loading directions.

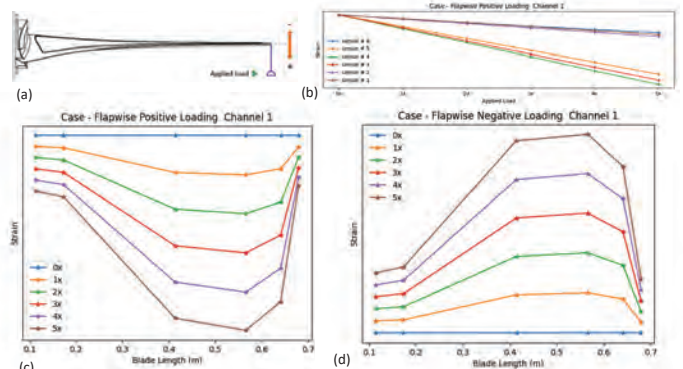


Figure 5(a) Schematic diagram illustrates the tip loading case of the blade. (b) Applied load vs measured strain by FBG sensors at discrete locations on the blade. Measured strain profile on the blade under positive (c) and negative (d) flapwise loading case.

Furthermore, effect of loading at different radial locations on the strain profile of the blade is shown in fig. 6. Load is applied at position A, B and C (as shown in fig 6(a)) in flapwise loading case of the blade. Fig 6(b) and (c) shows the impact of loading at given positions on the strain distribution at specific location on the blade. As the loading positions shifts towards the root of the blade, strain measured at sensors close to tip approaches zero strain. When blade is loaded at position B and C, sensor # 4, 5, 6 close to the tip shows similar strain results as can be seen as overlapping trend line, and is attributed to the limit of detection by the system.

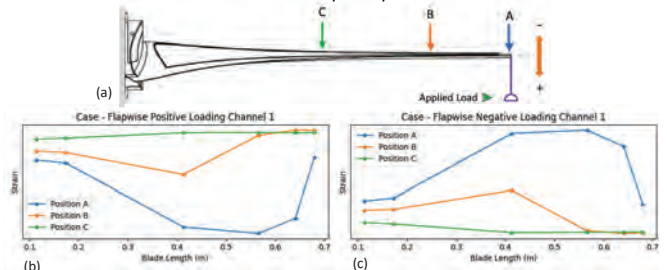


Figure 6(a) Schematic diagram showing the positions of the applied load on the blade. Graph shows change in strain profile with loading positions when load is applied in (b) positive and (c) negative direction.

## Conclusion

Fibre optic sensor system design and development of integrated system within nosecone of the tidal turbine discussed. Strain measurement at 24 discrete locations using FBG sensors for monitoring flapwise and edgewise loading conditions performed by using 4 sensor arrays. Test results on different loading conditions and its effects on strain profile of the blade is discussed.

Authors would like to thank the funding body EPSRC Supergen ORE Hub EP/S000747/1 and acknowledges contributions from all the project partners.

# Development of Fibre Optic Sensor System for monitoring unsteady loads on tidal turbine blade: Benchmarking Project

Dr Kaushal Bhavsar<sup>1</sup>, Miss Aananthya Sarma<sup>1</sup>, Dr Sam Tucker Harvey<sup>2</sup>, Dr Thomas Allsop<sup>1</sup>,  
Prof James Gilbert<sup>1</sup>, Prof Richard Willden<sup>2</sup>

<sup>1</sup>Faculty of Science and Engineering, University of Hull

<sup>2</sup>Department of Engineering Science, University of Oxford

## **Abstract**

Tidal stream turbines are exposed to challenging environmental conditions during their operation and are prone to complex steady and unsteady loads. Therefore, it is vital to understand the impact of such complex loading conditions on the tidal turbine blade and for the high-resolution data required. Fibre optic sensors offer several advantages in the measurement of such high-resolution data, especially in such harsh environmental conditions. They are small in size, immune to electromagnetic interference, chemically inert, and offer long-term reliability and multiplexing capability, i.e. several sensors can be integrated into a single optical fibre measuring different physical entities at discrete locations.

In a tidal stream turbine benchmarking project, a highly instrumented tidal turbine is developed with in-blade strain gauges and fibre optic sensors. This poster provides information about the design and development of an integrated fibre optic sensor (FOS) system for monitoring loads on the turbine blade. Considering size and space constraints for instrumentation on the turbine, a compact FOS system is developed for measuring flapwise and edgewise loads on the blade. The developed FOS system consists of a light source, interrogator and optical switch which are mounted in the nosecone of the turbine. Fibre Bragg Gratings (FBG) sensor arrays are used for strain measurement at 24 discrete locations. The measured strain profile over the blade length under different loading scenarios of the blade is discussed for one of the sensor arrays installed on the blade.

## INTRO AND BACKGROUND

This work focusses on **improving understanding of the effects of structural damping on the performance of wind turbine blades**. Damping is a phenomenon associated with the material, geometry construction and stiffness of a system. **Principal research partner SGRE has identified several uncertainties** associated with the experimental methodology for characterising damping in both composites samples and larger wind turbine blade assemblies. From observing these large uncertainties involved, a knowledge gap was found which triggered the motivation for this work.

My research aims to **produce an improved experimental methodology for the characterisation of material damping within composite materials**. This methodology will aid in the **development of an analytical model** and can be used to better understand the blade dynamics of a wind turbine. The developed model will be used in the **evaluation and development of current and future wind turbine blades**. In addition, the **effect of environmental condition will be investigated**, as there is an expected correlation between the damping of a system and the component condition.

## METHODOLOGY/TESTING PROCEDURES

### 1. DMA TESTING

Dynamic Mechanical Analysis (DMA) is a technique used to measure a wide range of material mechanical properties [1]. DMA considers the relationship between energy dissipation and the energy conserved within the material to determine the damping characteristics of a certain material.



On the Left, a typical DMA machine can be seen – the TA Q800 [2]. Within this experiment a three point clamp will be implemented as the test mode of choice, due to the high moduli values of the carbon composite samples.

During DMA testing, the influence of shear components is of particular interest. Through geometry optimisation, this phenomenon can be reduced to produce sensible damping results.

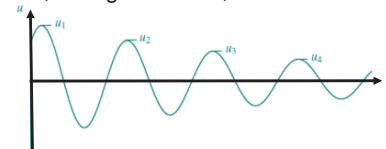
In addition to reducing shear influence, this geometry optimisation will be used to reduce the effect of multiple external influences, leading to more accurate damping characterisation.

### 2. LDM TESTING

The Logarithmic Decrement Method (LDM) is larger-scale method of determining the damping of a particular material/component [3]. The sample is pre-deformed to a specific amplitude and the samples recovery to its equilibrium position is monitored. A standard LDM setup can be seen below:



The logarithmic decrement may be found through measuring the amplitudes of two successive peaks, during oscillation, as shown below:



Through the following equation, the logarithmic decrement may be expressed as:

$$\delta = \ln \left( \frac{u_i}{u_{i+1}} \right) = \frac{2\pi\xi}{\sqrt{1-\xi^2}}$$

The response of the beam during the experiment is typically measured by accelerometers and the resultant data can be post-processed.

### 3. EMA TESTING

EMA is an experimental method that is used to characterise a material's modal properties [3]. This method, like LDM, is most commonly applied to large scale components. There are multiple options for the experimental methodology as shown below:

- |                            |                                     |
|----------------------------|-------------------------------------|
| <b>Excitation Options:</b> | <b>Data Acquisition:</b>            |
| • Modal Hammer             | • Accelerometers                    |
| • Shaker Table             | • Non-contact method (e.g. optical) |
| • Mobile Shaker            |                                     |

**Boundary Condition Options:**

- Fixed End
- Free End

An example of an EMA setup can be seen below:



Once the data acquisition has been post processed, there are many different mathematical toolboxes that can be used to characterise the damping of a selected component.

#### Advantages:

- Small scale testing
- Low frequency testing
- Investigate thickness, frequency and temperature effects

#### Disadvantages:

- Machine limitations (tensile test not possible)
- Shear component during 3 pt. bend test

#### Advantages:

- Simple test method

#### Disadvantages:

- Often overestimates damping
- Susceptible to many forms of external impact
- Mostly suitable for mode 1 evaluation

#### Advantages:

- Heavily developed test method
- Can target multiple modes
- Many variations of test available

#### Disadvantages:

- Large selection of post-processing tools

## FUTURE WORK

From conducting a detailed literature review, the current state of the research was found and gaps have been identified. Upon review, it has been possible to identify some future work that could also be carried out to increase the knowledge within the damping characterisation field. These main areas will be listed below:

- **Analyse the effect of aerodynamic damping – implement vacuum chamber**
- **Sample thickness/ aspect ratio – investigate the effect on out-of-plane damping components**
- **Understand the effect of the boundary condition – Fixed vs Free**
- **Frequency and temperature impact – DMA testing**
- **Develop a 3D analytical model for prediction of multi-orientation composite damping**

## REFERENCES

1. Menard et al, N., 2006. Dynamic mechanical analysis. Encyclopedia of Analytical Chemistry: Applications, Theory and Instrumentation.
2. Thermal Analysis: Dynamic Mechanical Analysis: DMA Q800, 2010.
3. Anil. K. Chopra, Dynamics of Structures: Theory and Applications to Earthquake Engineering, vol. Fourth Edition, 2015.

# Structural Damping Estimation of Wind Turbine Blades

*Euan Brough*

## Abstract

Growing demand for renewable power generation, in particular wind power, has pushed designers to scale up the size of these systems. At present, wind turbine blades are increasing in size to harness wind energy in the orders of multi-MW and there is no prospect to stop this growth. As the blades become larger, they become more flexible. With such vast development within the wind industry, all component manufacturers are striving to achieve improved performance and understanding of their components. As such, a deep knowledge of the structural dynamics of the blades for an economic design, which can provide the required service life, is inevitable.

This work focuses on the blade component of offshore wind turbines, where the length is greater than 100m. Previously, blades were made mostly of glass fibre-reinforced composites with some additional support. This makeup has historically been used in blades under 100m long, however, with the most recent blade developments exceeding 100m a new blade makeup is required. The newest generation of blades include carbon fibre composites, and the extent of their implementation will only increase as the demand for turbine growth increases.

The focus of this work is to understand the dynamic behaviour of the materials that make-up wind turbine blades, with a particular focus on carbon composites and the structural damping effect. Structural damping is the mechanism that dissipates the energy of the blade vibration. Any inaccuracies in the damping property has the potential to reduce the remaining useful life of these new composite blades. Further to this, the large-scale dynamic models will not be able to accurately predict the behaviour of the blades without first considering the effect of structural damping.

To determine this structural damping phenomenon, this work uses multiple different experimental methodologies, with the aim of producing an optimal methodology to characterise this phenomenon. Currently, the industry-standard method of testing for structural damping involves using Dynamic Mechanical Analysis (DMA) of a small material test coupon. DMA can provide decent estimates of a material's mechanical and dynamic properties. However, concerns surrounding the errors associated with the results have been raised, which were investigated. DMA is traditionally more applicable for use on materials with lower stiffness where the contribution of the shear stress is kept low.

An alternative method has been identified, which will be the focus of this work and will be compared with results from DMA to reduce the errors associated with structural damping results, namely the shear damping components. Experimental Modal Analysis (EMA) involves studying the dynamic behaviour of a structure. This free-free testing methodology will be completed both in atmospheric and vacuum conditions, with the aim of removing damping contributions caused by aerodynamic damping. This will provide useful insight into the isolated structural damping and aerodynamic damping contributions for different strain levels within the medium-scale test samples.

# OPPORTUNISTIC MAINTENANCE FOR SCOTWIND SITES

The historic ScotWind leasing round saw 25 GW being allocated, with 11 GW allocated to floating offshore wind (FOW) sites. However, many of these sites are in previously untapped areas which are remote, deep and far from shore. This work analyses the met ocean conditions at site and makes recommendations for maintenance strategy for the future developments

**AUTHORS**  
Jade McMorland<sup>1</sup>, Prof. Maurizio Collu<sup>1</sup>, Dr. David McMillan<sup>1</sup>, Dr. James Carroll<sup>1</sup> and Dr. Andrea Coraddu<sup>2</sup>.

**AFFILIATIONS**  
University of Strathclyde  
<sup>2</sup>TU Delft

## INTRODUCTION



ScotWind saw 25 GW being leased in the West, North, North East and East regions of Scottish Waters [1].

These sites are due to become operational around 2030 and will be a huge addition to the exciting Scottish fleet of offshore wind farms.

## OPERATIONAL CHALLENGES

These sites present a new set of operational challenges:

- ❖ Average distance of 70 km from mainland
- ❖ Previously untapped areas
- ❖ Remote locations with no existing infrastructure
- ❖ Deep water floating sites

## OPERATIONAL STRATEGIES

O&M can account for 1/3 of the cost of energy [2] and therefore plays an important role in ensuring future sites remain economically viable. Therefore, new strategies must be explored

A new strategy being explored is defined as "opportunistic maintenance" (OM).

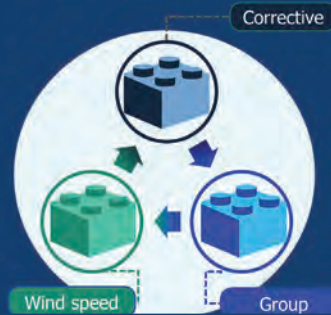


## OPPORTUNISTIC MAINTENANCE

OM allows for additional maintenance actions to be carried out based on "opportunities" at site [3].

There are three main types of "opportunities" where maintenance is performed

- 1) Corrective-based: performing scheduled maintenance during corrective maintenance activities
- 2) Wind speed based: maintenance is performed when wind speed is low as income is low
- 3) Group-based: scheduled maintenance tasks are "grouped"



Benefits include:

- ✓ sharing of resources
- ✓ effective use of weather windows
- ✓ decreased downtime and savings in operational expenditure (OpEx)

However, existing literature fails to address the practical implications of such a strategy such as:

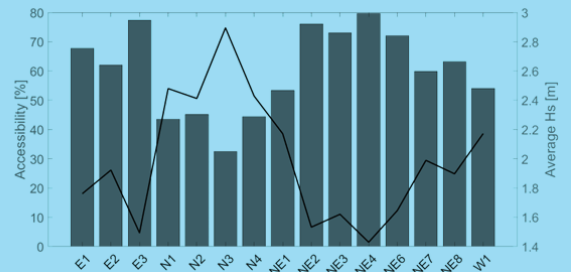
- x Existing met-ocean limits on access
- x Additional time at site required
- x Impact on downtime

## SCOTWIND MET OCEAN ANALYSIS

In order to determine if an OM strategy is viable, the conditions at site must first be analysed. Time Based Accessibility (TBA) is a measure of ease of access to the site. This is calculated based on the ERA 5 dataset.

Sites in the N and W regions see a reduced accessibility compared with other areas.

While TBA gives an indication of site accessibility, it does not consider the "lengths of access" available, known as weather windows.



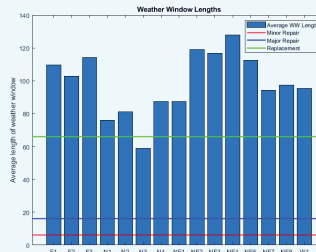
## WEATHER WINDOW PROFILES

The weather window model determined the length of access available at each time-step in the input data. Therefore, one "block" of access can contain multiple weather windows of varying lengths.

Access is further limited by weather window requirement which is dependent on



Weather windows which do not meet the required length are now viewed as periods of no access. OML length is the increased length due to additional maintenance actions



The result show, that while overall access to site is low, the existing periods of access are much longer than the time required for a minor or major repair.

The average length of access across all sites is found to be 30 hours – allowing for multiple maintenance actions to take place.

However, there is a balance between length of weather window and length of waiting time for such a window.

For an OM strategy to be beneficial



## CONCLUSIONS

- 1 Weather window profiles across all sites would allow for an OM strategy
- 2 OML will limit the cost effectiveness of an OM strategy due to additional downtime cost
- 3 Cost benefit analysis required to determine the maximum OML where cost of waiting will be less than the transport savings
- 4 OML will determine the type of additional activities which can take place

## REFERENCES

- [1] Crown Estate Scotland. "ScotWind offshore wind leasing delivers major boost to Scotland's net zero aspirations." *Crown Estate Scotland* (2022).
- [2] Global Wind Energy Council. "Global Offshore Wind: Annual Market Report 2020." *Global Offshore Wind Report* (2020).
- [3] Besnard, Francois, et al. "An optimization framework for opportunistic maintenance of offshore wind power system." *2009 IEEE Bucharest PowerTech*. IEEE (2009)

## **OPPORTUNISTIC MAINTENANCE FOR SCOTWIND SITES**

Jade McMorland

University of Strathclyde

The historic ScotWind leasing round saw 25 GW of offshore wind capacity being allocated, with 11 GW allocated to floating offshore wind (FOW) sites. However, many of these sites are in previously untapped areas which are remote, deep and far from shore. The additional complexities of floating sites, due to turbine motion, further limit the already challenging accessibility of these sites. Therefore, a flexible, and cost-effective, maintenance strategy is required. One such proposed strategy is opportunistic maintenance (OM). This strategy performs additional maintenance tasks during periods of “opportunity” such as low wind and economically favourable periods, during existing corrective maintenance trips or grouping together preventive maintenance tasks. This has the advantage of making effective use of scarce weather windows and sharing transport costs between multiple maintenance actions. However, the existing literature fails to address the practical considerations required for such a maintenance strategy.

The application of OM requires a prolonged period at the site and therefore requires a longer weather window. This work examines the met-ocean conditions and weather window profiles of the ScotWind zones. It highlights the relationship between significant wave height and time-based accessibility and provides details of the duration of access across the 15 ScotWind zones. Results indicate that an opportunistic-based maintenance strategy is possible, however, this will incur an additional waiting time due to the correlation between length of access and length of waiting time.

# Modelling of a Wave Energy Converter Power Take-off, Considering Power Limiting Operation

X. Zhang, J. Apsley, M. Iacchetti, Z. Liao

## Introduction

Wave energy is a promising renewable energy resource. A multi-float platform wave energy platform (M4) has been designed by the University of Manchester for capturing wave energy. Tank tests have shown the M4 has a high capture width ratio. Project EPV0405101 addresses minimum levelized cost of energy from wave to wire. This poster summarises the work on power limiting operation, which determines PTO sizing and capital costs.

## Power take-off

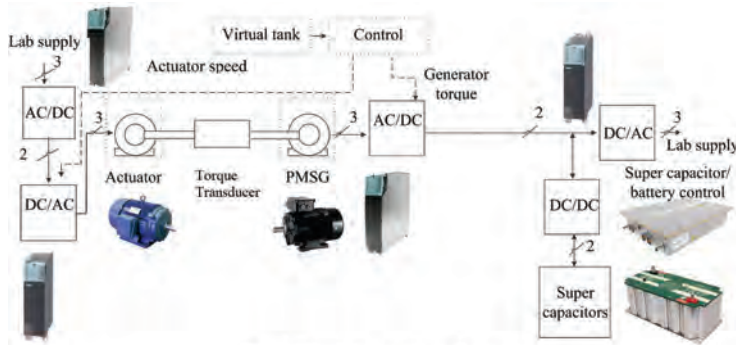


Fig. 1 Emulation system diagram

The lab-scale, electrical power take-off (PTO) in Fig. 1 is under construction, to allow dry test of control algorithms (G. Li, QML). The actuator emulates the M4 multi-float platform dynamics, controlled by virtual tank simulation in the dry test at kW scale, with multi-directional wave prediction (M. Belmont, Exeter). For power limiting operation, the PMSG generator is controlled as a linear damper. The super capacitors and bidirectional DC/DC converter on the DC link absorb power at high wave peaks and regenerate at low wave power to provide power smoothing. PQ control on the grid side converter will allow power transmission from the DC link to grid.

## 'M4' Wave energy platform

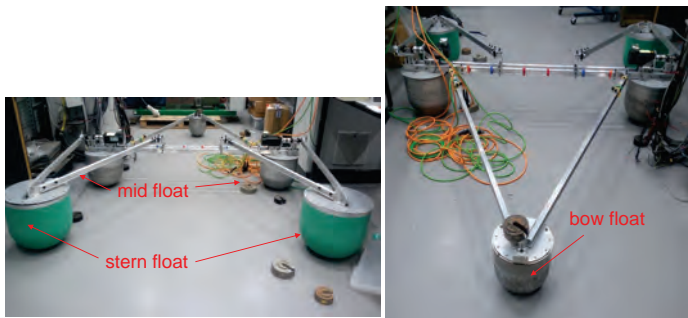


Fig. 2 M4 two-channel platform

Fig. 2 shows the 2W, tank-scale M4 platform with two floating output channels in a 1-2-2 configuration with one bow float, two mid and two stern floats, used to validate the hydrodynamic models in the PTO Simulink model. Additional floats will give three channels of power take-off (P. Stansby, S. Draycott, Manchester).

## Generator/converter power limits

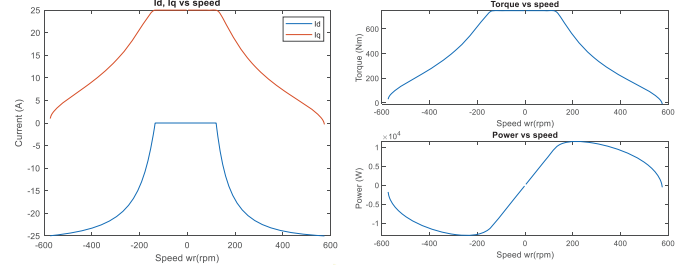


Fig. 3 Generator/converter operating power limits

The generator and its converter have limits on current which constrains generator torque, and on voltage which constrains speed. The speed range can be extended using field weakening current  $I_d$ , but this reduces the torque capability at high speeds (set by current  $I_q$ ) as shown in Fig. 3. These limits are being used to optimize power take-off component selection.

## Generator control

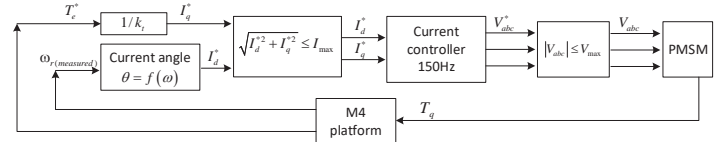


Fig. 4 Generator controller block diagram

The generator controller is shown in Fig. 4. The torque reference for the PMSG generator is derived from the M4 platform speed, with a linear damping algorithm. PMSG measured torque and speed are fed back to the M4 controller. Fig. 5 shows power limiting operation of the generator with the constraints applied from Fig. 3, where the voltage limits applies when the PMSG is operating in the field weakening region. For illustration, the more effective linear non-causal optimal control algorithm is used for Fig. 5.

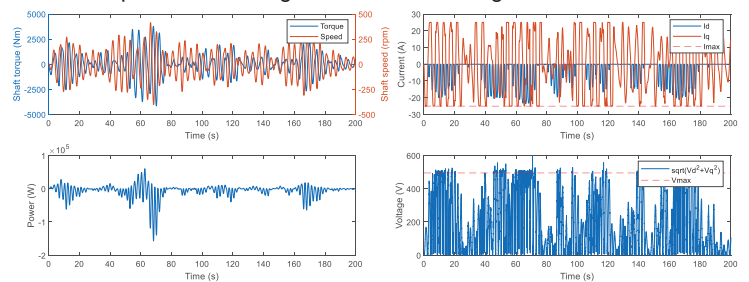


Fig. 5 Torque, speed, power from wave and operating limits plots from PMSG

## Generator over-speed protection

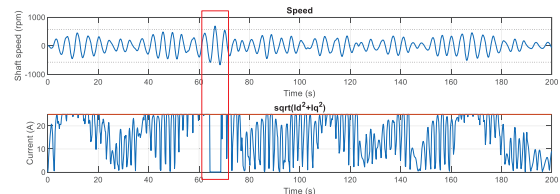


Fig. 6 Overspeed protection for generator at peak wave

High generator terminal voltage resulting from extreme waves could damage power electronic devices, so over-speed protection is required. Fig. 6 shows simulation of a soft switch-off, where the generator is temporarily disconnected from the converter, giving zero current. A complete shutdown will be implemented in high sea states.

# Modelling of a Wave Energy Converter Power Take-off, Considering Power Limiting Operation

## *Abstract*

Wave energy is a promising renewable energy resource, but still not commercialized due to its high unit cost for electric power generation, when compared against other types of renewable energy resources, i.e. wind and solar power [1].

A multi-mode multi-float platform wave energy platform (M4) has been designed by the University of Manchester for capturing wave energy. Tank tests have shown the M4 has a high capture width ratio, and linear non-causal optimal controller has been designed to maximize power capture for M4 [1].

This project addresses the electrical power take-off, developing and optimizing control algorithms for a multi-channel wave energy converter, in order to minimise levelized cost of energy from wave to wire. The wave-to-wire lab system will emulate the prime mover for wave energy, and build hardware system for electric power generation (PMSM generator, power conversion systems, energy storage and grid interface).

This poster summarises the work on power limiting operation, which determines PTO sizing and capital costs, targeting the generator design/control, DC/DC converter control and grid side inverter controls.

[1] Z. Liao, N. Gai, P. Stansby and G. Li, "Linear Non-Causal Optimal Control of an Attenuator Type Wave Energy Converter M4," in *IEEE Transactions on Sustainable Energy*, vol. 11, no. 3, pp. 1278-1286, July 2020, doi: 10.1109/TSTE.2019.2922782.

# Conjunctive operation of tidal lagoons and its interaction study

## Introduction

- Despite the great advantages of tidal lagoons, such as predictable renewable energy generation and flood risk reduction, tidal lagoons are expected to have drawbacks like environmental impacts and intermittent power generation (Adcock et al., 2015).
- The conjunctive operation of multiple Tidal Range Schemes (TRSs) may partially offset the energy output intermittency of a single TRS (Neill et al., 2016).
- This research aims to evaluate the potential interactions between TRSs on the hydrodynamic environment and electricity generation.



Fig. 1. The layout of the turbine housing and sluice gate blocks around (a) North Wales Tidal Lagoon (NWTL); (b) West Somerset Lagoon (WSL); (c) Swansea Bay Lagoon (SBL).

## Methods

- Hydrodynamic model TELEMAC-2D has been refined to model tidal lagoons.
- Full momentum conservation between the subdomains is achieved (Guo et al., 2021).
- Independent operation of the turbines and sluice gate blocks.
- Two different hydrodynamic model were applied, that are Continental Shelf (CS) model, as well as Severn Estuary and Bristol Channel (SEBC) model.
- Each lagoon was operated individually and then conjunctively to explore the potential interaction.

## References

Adcock, T. A. A., et al., 2015. Tidal power generation - A review of hydrodynamic modelling. *Proceedings of the Institution of Mechanical Engineers, Part A: Journal of Power and Energy*, 229(7), pp.755-771.  
Guo, B., et al., 2021. Refined hydro-environmental modelling for tidal energy generation: West Somerset Lagoon case study. *Renewable Energy*, 179, pp.2104-2123.  
Neill, S. P., et al., 2018. Tidal range energy resource and optimization - Past perspectives and future challenges. *Renewable Energy*, 127, pp.763-778.

## Results

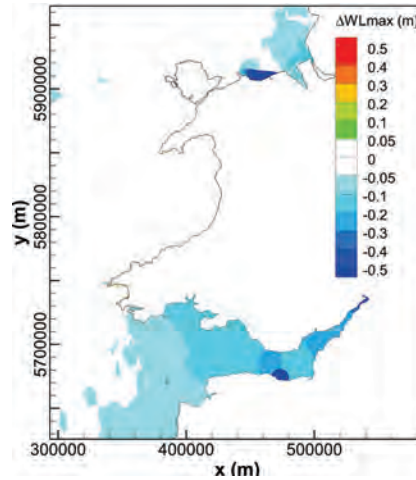


Fig. 2: The combined impact of the NWTL and WSL on maximum water level.

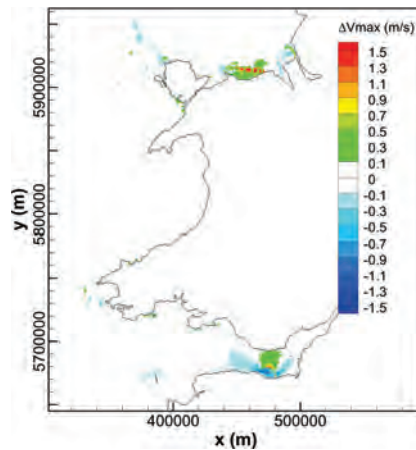


Fig. 3: The combined impact of the NWTL and WSL on maximum velocities.

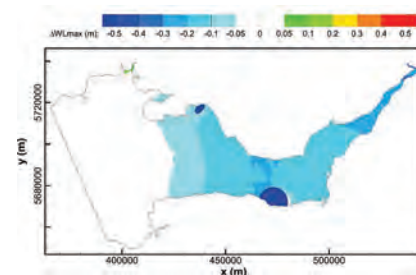


Fig. 4: The accumulative impact of SBL and WSL on the maximum water level.

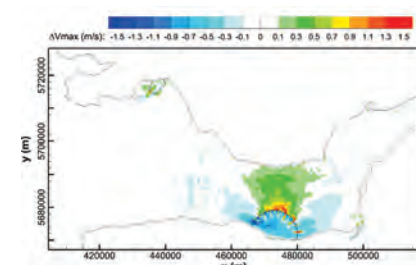


Fig. 5: The accumulative impact of SBL and WSL on maximum velocities.

Table 1: Energy outputs for the WSL and NWTL in the CS model

TRS	Condition	Flexible two-way generation (GWh)
NWTL	Individual operation	195.04
	with WSL	194.11
	difference	-0.48%
WSL	Individual operation	219.46
	with NWTL	222.97
	difference	1.6%

Table 2: Energy outputs for the WSL and SBL in the SEBC model.

TRS	Condition	Flexible two-way generation (GWh)
WSL	Individual operation	233.48
	with SBL	231.84
	difference	-0.76%
SBL	Individual operation	23.74
	with WSL	22.87
	difference	-3.7%

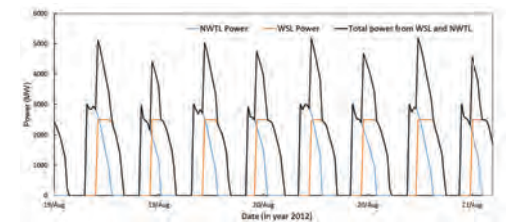


Fig. 6: The power output from WSL and NWTL with the conjunctive optimised two-way operation.

- In the conjunctive operation of WSL and NWTL, as well as WSL and SBL, the hydrodynamic interactions between the lagoons were found to be minor (Fig. 2 – Fig. 5).
- The operation of WSL could slightly decrease the tidal range in the Swansea Bay thus reduce the electricity generation of SBL, while the operation of NWTL has the opposite effect on WSL power generation (Table. 1 and 2).
- The intermittency of individual TRS power output was reduced from 2.5-3.75 h to less than 1.5 h with jointly operating (Fig. 6).

## Conclusion

- The interactions between the lagoons are associated with the lagoon scale, location, tidal phase, et al. Therefore, a general conclusion could not be obtained.
- The feasibility of relatively continuous tidal power output is presented for the conjunctive operation of WSL and NWTL.

# The conjunctive operation of tidal range energy scheme on the west coast of the UK

Bin Guo<sup>\*</sup>, Reza Ahmadian<sup>\*</sup>, Roger A Falconer

*School of Engineering, Cardiff University, The Parade, Cardiff CF24 3AQ, UK.*

*Corresponding author: Reza Ahmadian, Queens Building, Cardiff University, 5 The Parade, Roath, Cardiff, U.K. CF24 3AA. Email: Guob2@cardiff.ac.uk*

## Abstract

---

Despite the great advantages of tidal lagoons, such as predictable renewable energy generation and flood risk reduction, tidal lagoons are expected to have drawbacks like environmental impacts and intermittent power generation, while the conjunctive operation of multiple Tidal Range Schemes (TRSs) may partially offset the energy output intermittency of a single TRS. This paper studied the potential interactions between TRSs on the Hydrodynamic environment and electricity generation, including North Wales Tidal Lagoon (NWTL), West Somerset Lagoon (WSL) and Swansea Bay Lagoon (SBL). Each lagoon was operated individually and then conjunctively to explore the potential interaction on the hydrodynamic impact and power output. In the conjunctive operation of WSL and NWTL, as well as WSL and SBL, the interactions between the lagoons were investigated but found to be minor. Following the interaction on water level, variations in power generation were also observed. Overall, the interactions between the lagoons are associated with the lagoon scale, location, tidal phase, et al. Therefore, a general conclusion could not be obtained. However, the feasibility of relatively continuous tidal power output is presented for the conjunctive operation of WSL and NWTL, and the intermittency of individual TRS power output was reduced noticeably.

**Keywords:** Tidal energy; Tidal lagoon; environmental impact; conjunctive operation; interaction

---

# Short design waves for semi-sub FOWTs experiencing viscous drift



UNIVERSITY OF PLYMOUTH

Tom Tosdevin<sup>1\*</sup>, Dave Simmonds<sup>1</sup>, Martyn Hann<sup>1</sup>, Deborah Greaves<sup>1</sup>

<sup>1</sup> University of Plymouth, Plymouth, United Kingdom

\*Corresponding email: [tom.tosdevin@postgrad.plymouth.ac.uk](mailto:tom.tosdevin@postgrad.plymouth.ac.uk)



## Abstract

Results from physical experiments using a 1:70 scale model of a semi-sub floating wind turbine, the VoltturnUS-S, are presented. A comparison of extreme mooring loads produced using irregular waves, constrained response conditioned focused waves and constrained wave groups consisting of 2 large peaks are given. It is shown that constrained wave groups efficiently produced extreme responses more in line with those from extended irregular waves series than could be achieved using conditioned focused waves.

**Keywords:** floating wind, drag, viscosity, focused waves, constrained focused waves, rare wave groups.



Fig.1 Photo of 1:70 scale model

The extreme sea state studied had the turbine in idling conditions (no thrust from turbine) and was modelled with a JONSWAP spectrum with  $H_s = 12\text{m}$ ,  $T_p = 14.4\text{s}$  and  $\gamma = 3.3$ . 18, one hour irregular wave seeds were run and the 18 largest mooring loads generated are plotted in Fig.2 along with the average surface elevations and responses given by the thick lines. The extreme loads were caused by a sequence of 2 large waves.

## 1. Device

The data presented in this work is for a 1:70 scale model semi-sub design; the VoltturnUS-S platform and IEA 15MW reference turbine [1,2] shown in Fig.1. The physical experiments were conducted at the COAST lab at the University of Plymouth. The mooring consisted of 3 catenary chains and all waves were unidirectional. The mooring loads studied were at the fairlead on the front column.

## 2. Long sequence irregular wave approach

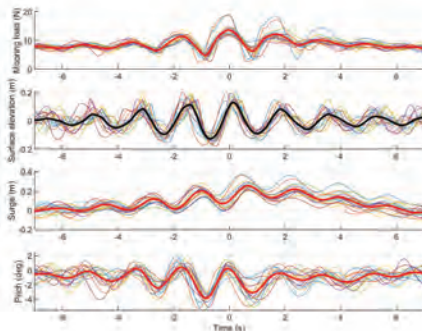


Fig.2 Empirical extremes in irregular waves

## 5. Rare wave groups

A derived process  $z_k$  was defined in [5] to search a surface elevation time series for wave groups which might bring on the occurrence of parametric roll of container ships. They were found to occur for large values of  $z_k$ .

$$z_k(t) = \sum_{p=1}^k \eta(t + (p-1)\tau) \quad (1)$$

Where  $\tau$  is a predefined period of interest, which is in this work set to the peak period of the sea state ( $T_p$ ), and  $k$  is the wave group index indicating the number of large peaks (2 in this instance). In [6] the occurrence of these rare wave groups was studied using wave buoy data and the average wave profile for a group of  $k$  large peaks, conditioned on the  $k$ th derived process being a maximum, was found to be proportional to the sum of  $k$  autocorrelation functions of the wave elevation ( $r_{\eta\eta}$ ), separated in time by  $(p-1)\tau$ ,  $p = 1 \dots k$ .

$$E[\eta(t)|z_k(0)] = \frac{\hat{z}_k(t)}{\sigma_{z_k}^2} \sum_{p=1}^k r_{\eta\eta}(t_p) \quad (2)$$

If  $k = 1$ , the NewWave is generated. The surface elevation of the wave group at 0 seconds based on 2 large peaks ( $k=2$ ) was constrained into 20 short random irregular backgrounds. The amplitude was scaled to the 99th percentile of  $z_k$  rather than the most probable maximum (~38th percentile) in line with a constrained focused wave methodology outlined in [7]. A comparison of the single wave group (G2), constrained wave groups (CG2) and the empirical extreme profile from the irregular waves is given in Fig.4.

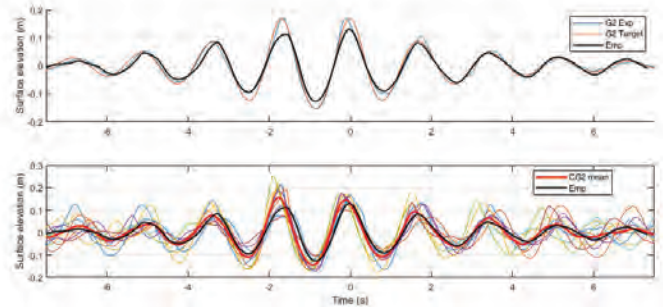


Fig.3 Empirical average wave profile (Emp) comparison with G2 (upper) and CG2 (Lower)

## 3. Short sequence constrained focused wave approach

### What are focused / constrained focused waves?

Focused waves focus wave components by linear dispersion to produce the shape of an extreme wave. These waves can be constrained into short irregular wave time series.

### Why constrained focused waves over single focused waves?

Low frequency surge motions make an important contribution to the mooring load and so a series of preceding waves need to be modelled before the focused wave event.

### What is a response conditioned focused waves?

The shape of the wave is conditioned on the linear response amplitude operators (RAOs) to give the shape of the wave most likely to produce the extreme of the response of interest. The single focused wave is termed the most likely extreme response wave (MLER) and the constrained version the conditional random response wave (CRRW).

### What are the advantages of short design waves over irregular waves?

Constrained focused waves have the potential to reduce simulation times significantly compared with irregular waves. They are also short enough that they may be used in computationally expensive, high fidelity numerical modelling.

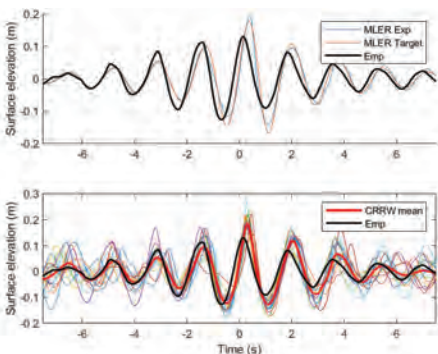


Fig.3 shows how the empirical average wave profile found (Emp) to produce the extreme mooring loads in Fig2 did not match that of the response conditioned focused wave (MLER and CRRW). These profiles were found to produce lower extreme mooring loads than those measured in the irregular waves (Fig.5).

Fig.3 Empirical average wave profile (Emp) comparison with MLER (upper) and CRRW (Lower)

## 6. Extreme responses

Fig.5 shows how the 20 CG2 profiles produced extreme mooring loads comparable to those from the 18 long irregular wave series. However the 15 CRRWs generated no upper percentile responses.

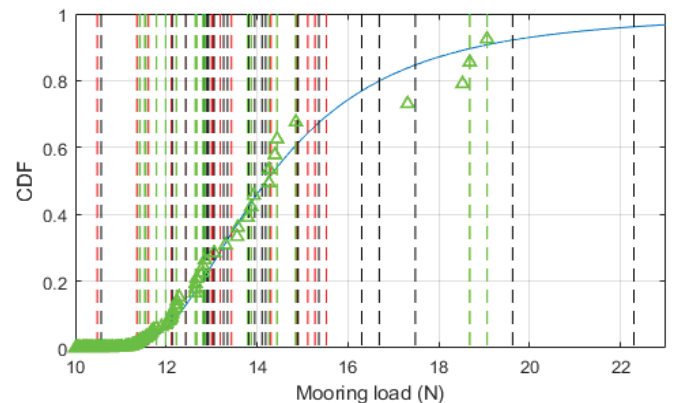


Fig.5 Comparison of load values. Irregular waves (green, dashed); CG2 (black, dashed); CRRWs (red, dashed). Response peak values and CDF from irregular wave series (green triangles).

## 4. Viscous drift

The extreme surge positions and mooring loads of semi-subs have been found to be caused by viscous drag [3]. This is observed to be a 3<sup>rd</sup> order effect (proportional to the wave amplitude cubed) primarily acting above the mean still water line [4]. This explains why the focused waves conditioned on the linear RAOs did not match the shape of the average wave leading to the extreme mooring loads in the irregular waves.

## Conclusions

The use of constrained wave groups consisting of an arbitrary number of large peaks was shown to efficiently reproduce extremes of surge and mooring load response in semi-submersible FOWTs where viscous drift effects are important.

## References

- [1] E. Gaertner et al., "Definition of the IEA wind 15-megawatt offshore reference wind turbine tech. rep.", 2020.
- [2] C. Allen, A. Viscelli, H. Dagher, A. Goupee, E. Gaertner, N. Abbas, M. Hall, and G. Barter, "Definition of the umaine voltturnus-s reference platform developed for the IEA wind 15-megawatt offshore reference wind turbine", National Renewable Energy Lab.(NREL), Golden, CO (United States), Tech. Rep., 2020.
- [3] L. Wang, A. Robertson, J. Jonkman, Y.-H. Yu, A. Koop, A. B. Nadal, H. Li, E. Bachynski-Polić, R. Pinguet, W. Shi et al., "Oc6 phase Ib: Validation of the CFD predictions of difference-frequency wave excitation on a fowt semisubmersible," Ocean Engineering, vol. 241, p. 110026, 2021.
- [4] S. Ma, D.-k. Xu, W.-y. Duan, J.-k. Chen, K.-p. Liao, and H. Wang, "The numerical study of viscous drag force influence on low-frequency surge motion of a semisubmersible in storm sea states," Ocean Engineering, vol. 213, p. 107511, 2020.
- [5] D.-H. Kim and A. W. Troesch, "Statistical estimation of extreme roll responses in short crested irregular head seas," in SNAME Maritime Convention. OnePetro, 2013.
- [6] H. Seyffert, D.-H. Kim, and A. W. Troesch, "Rare wave groups," Ocean Engineering, vol. 122, pp. 241–252, 2016.
- [7] T. Tosdevin, S. Jin, D. Simmonds, M. Hann, and D. Greaves, "On the use of constrained focused waves for characteristic load prediction", RENEW, 2022.

## **Short design waves for semi-sub FOWTs experiencing viscous drift**

*Tom Tosdevin, University of Plymouth*

Results from physical experiments using a 1:70 scale model of a semi-sub floating wind turbine, the VoltornUS-S, are presented. The 50 year extreme storm at a site off the coast of Maine in the USA was used for the wave conditions, as the turbine would be idling, the wind loading was neglected. A comparison of extreme mooring loads produced using irregular waves, constrained response conditioned focused waves and constrained wave groups consisting of 2 large peaks are given. It is shown that constrained wave groups efficiently produced extreme responses more in line with those from extended irregular waves series than could be achieved using response conditioned focused waves. This is thought to be due to the importance of 'viscous drift' for semi-subs which is an increase in the low frequency surge motions of the model due to viscous drag not captured by linear response amplitude operators.

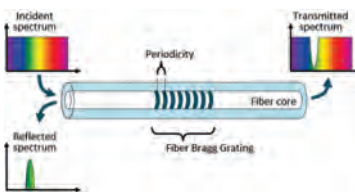


## Background & Motivation

Fiber Bragg Grating (FBG) sensors for structural health monitoring (SHM) for wind turbine blades (WTB) is a mature and highly developed technique. While a typical SHM system has its own benefits/features, defect detection in WTB come with a lot of challenges as damage is not a physical parameter, rather a local change in the material's properties or at the structure boundaries that degrades structural performance [1]. These depend on sensor positioning & lengths, sensitivity and resolution of measurements. To simply investigate this small variations in strain, static loading tests of cantilever Al beam with a known defect present mounted with FBGs measuring strain has been conducted. The experiment results are compared with FEA simulations from ANSYS. A LabVIEW based DAQ for the wavelength division multiplexed (WDM) FBGs have been used to analyse the results with a peak detection/ Gaussian fit algorithm developed to improve the resolution.

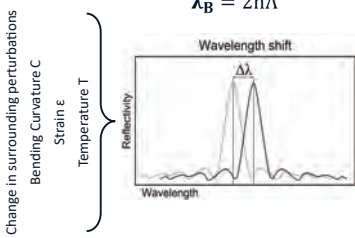
## Fibre Optic Grating Based Sensors: Working Principle

**Grating:** a short segment with a **Periodic Perturbation of Refractive Index** along



$\lambda_B$ : Bragg Wavelength  
n: Refractive Index of the core  
 $\Lambda$ : Period of the grating

$$\lambda_B = 2n\Lambda$$

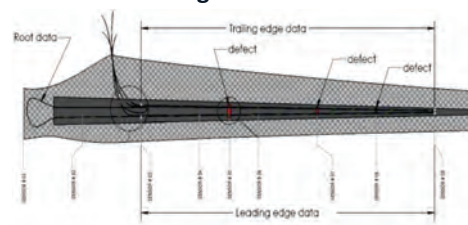


When FBG is subjected to strain, the reflected wavelength shifts left/ right proportional to the applied strain based on tension/ compression respectively.

$\Delta\lambda_B$ : Wavelength Shift  
 $p_e$ : strain optic coefficient  
 $\epsilon$ : Strain

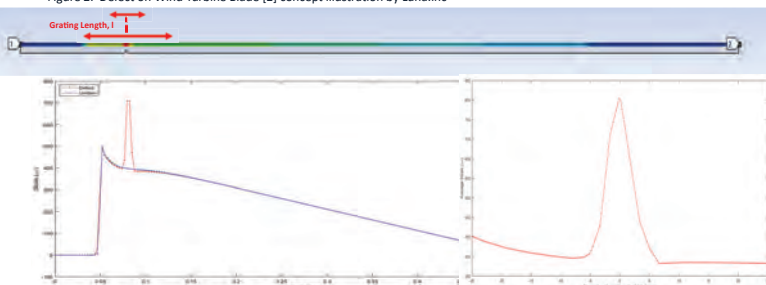
$$\frac{\Delta\lambda_B}{\lambda_B} = (1 - p_e)\epsilon$$

## FEA Static Loading Simulation for Defective Beam



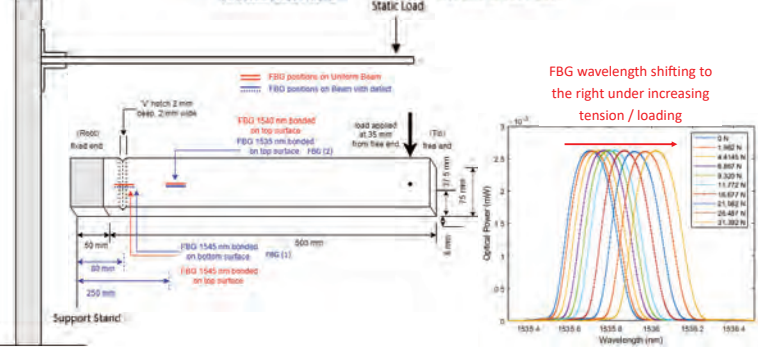
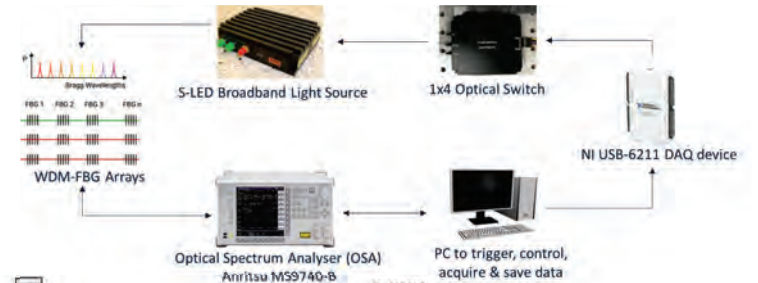
As Blades are large, complex structures, predicting defect behaviour can be difficult, to simplify this, preliminary studies are done on a Aluminium beam with & without defects.

Figure 2: Defect on Wind Turbine Blade [2] concept illustration by Luna.Inc

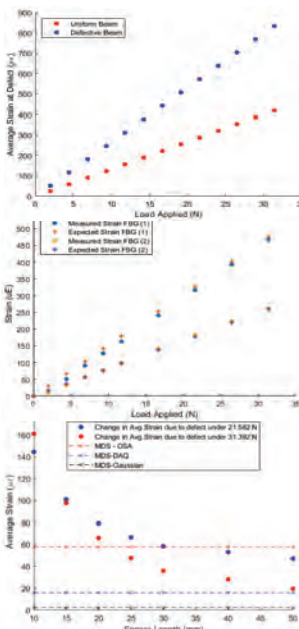


Simulations conducted for both a uniform (defect-less) and a defective beam and also for various sensing lengths mounted at defect to measure strain under increasing transverse loading.

## Data Acquisition System & Experiment Set-Up



## Defect Detection Results & Discussion



- Average strain experience by FBGs bonded at the defect location is higher than that of the FBGs bonded at the same location in the Uniform Beam. Using a peak/ Gaussian fitting algorithm, the resolution were increased up to 1  $\mu\text{m}$  which is  $\approx$  1-2.5  $\mu\epsilon$ .
- Depending on mounting location, the FBGs experience tension/compression during experiments as expected and show good agreement with the FEA expected strain.
- FEA results for different sensing lengths considered for simulations at defect location and the change in avg. strain due to defect are well above the minimum detectable strain (MDS) of  $\sim$  16.7  $\mu\epsilon$  for the limited OSA-DAQ conditions used and 2.5  $\mu\epsilon$  MDS determined by the Gaussian fit respectively.

## Conclusions & Future Work

This work has demonstrated a method of using WDM-FBGs to characterize defects based on strain measurements using precise mounting locations. Expected strain from FEA vs Experimental FBG strain measured show good agreement, while sensing length vs avg strain FEA investigation has shown promising solution towards determining the sensing lengths for a given defect & load case. For future work, load-strain tests will be done on composite beams/ scaled blades with & without defects of various sizes as the above FBG sensor network can further be expanded to understand the significance of distributed sensing of blades and trade-off between sensor position/ length and sensitivity and resolution.

**Acknowledgements:** The authors would like to thank Supergen and acknowledge that this work has been facilitated by the EPSRC Supergen ORE Hub EP S 000747-1 Grant

## References

- [1] Guemes, A., Fern'andez-L'opez, A., Diaz-Maroto, P. F., Lozano, A., and Sierra-Perez, J. (2018). "Structural health monitoring in composite structures by fiber-optic sensors". In: Sensors 18.4, p. 1094.
- [2] Fibre Bragg Grating Reference Image taken from: <https://hittech.com/en/portfolio-posts/horia-the-fiber-bragg-grating-manufacturing-solution/>
- [3] Luna Case Study: Using HD-FOS for Defect Detection in Wind Turbine Blades During Fabrication and Testing, <https://lunainc.com/sites/default/files/assets/files/resource-library/CASE-STUDY-HDFOS-for-Wind-Turbine-Blade-Test-May-18th-2016.pdf>

# Multi-Point Sensing of Wind Turbine Blade Loading for Structural Health Monitoring and Defect Detection

Aananthy S Sarma, James M Gilbert

*School of Engineering, University of Hull*

Fibre Bragg Grating (FBG) sensors for structural health monitoring (SHM) for wind turbine blades (WTB) is a mature and highly developed technique [1]. While a typical SHM system has its own benefits/ features, defect detection in blades come with a lot of challenges as damage is not a physical parameter, rather a local change in the material's properties that degrades structural performance [2]. These defects or small variations in parameters such as strain which lead to defects are much harder to detect with present SHM systems with limited resolution and sensitivity. Improving the resolution of measurements and investigating the use of these sensors at different points along the blade (multi-point sensing) is important to WTB-SHM research. Blades are large scale, geometrically complex and constructed from composite materials with complex structural properties, making predictions of behaviour difficult. As a step towards studying defects on these structures, tests have been conducted on an Aluminium cantilever beam with a known defect since the blades can be viewed as beam-like structures a numerical calculations' perspective.

Some of the main concerns in utilising FBGs for large structures are the sensitivity to change in strain due to the presence of a defect, resolution of measurements, sensing length/ no of sensors and suitable data interrogation technique. A finite element analysis (FEA) using ANSYS v19.2 was carried out in simulation to investigate the load-strain relationship and strain distribution along the beam as well as determining the optimum FBG sensor length for a given defect, which was a 2 mm deep, 2 mm wide 'V' notch on top of the beam at 30 mm from the fixed end. Experiments were conducted both for a beam with this defect as well as a uniform (defect-less) to compare changes in measured strain due to the defect.

The minimum detectable strain (MDS) or limit of strain detection for this experimental setup using the optical spectrum analyser (OSA) as the interrogator were estimated at  $58.3 \mu\epsilon$ . With a span of 2 nm for each FBG peak spectrum and sampling points of 1001, the OSA's in-built fitting function caps the MDS at approximately  $16 \mu\epsilon$ . Using a LabVIEW based data acquisition system (DAQ) developed for wavelength division multiplexed (WDM) FBGs and a peak detection-Gaussian fitting algorithm, results from both simulations and experiments were compared. FBG wavelengths shifts of up to 1 pm were detectable during post processing, which correspond to strain variations up to 1-2.5  $\mu\epsilon$  for FBGs with a strain sensitivity of 1.2 pm/ $\mu\epsilon$ . Additional studies on average strain expected by different sensing/ grating lengths under various loading have been completed and it can be seen that the change in strain expected for defective beam vs uniform defect-less beam are well above the MDS values posed by the interrogator and experiment setup. Another observation is that as grating length increases, the average strain due to the presence of defect nearly matches the average strain measured at the same location for the beam without the defect. Preliminary results from these investigations indicate that this WDM-FBG system can further be expanded and serves to understand the trade-off between sensor positioning, importance of utilising optimum sensing lengths and number of sensors required for distributed load /strain monitoring and defect detection. This will be validated by further experiments in future.

[1] Glavind, L., Olesen, I. S., Skipper, B. F., and Kristensen, M. V. (2013). "Fiber-optical grating sensors for wind turbine blades: a review". In: *Optical Engineering* 52.3, p. 030901.

[2] Guemes, A., Fernandez-Lopez, A., Diaz-Maroto, P. F., Lozano, A., and Sierra-Perez, J. (2018). "Structural health monitoring in composite structures by fiber-optic sensors". In: *Sensors* 18.4, p. 1094.

# Wind farm parameterisation in WRF

Karim Ali<sup>a</sup>, Timothy Stallard<sup>a</sup>, David M. Schultz<sup>b,c</sup>, Alistair Revell<sup>a</sup>, and Pablo Ouro<sup>a,b</sup>

<sup>a</sup> School of Engineering, University of Manchester, UK

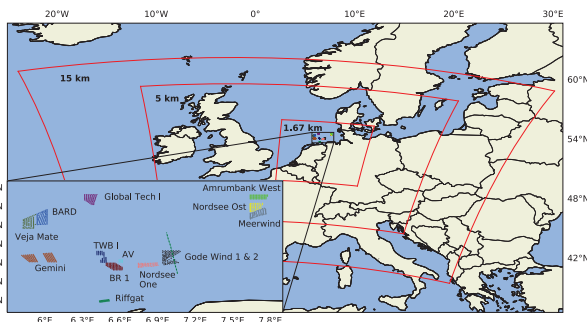
<sup>b</sup> Centre for Crisis Studies & Mitigation, University of Manchester, UK

<sup>c</sup> Centre for Atmospheric Science, Department of Earth & Environmental Sciences, University of Manchester, UK

The United Kingdom (UK) is aiming at achieving carbon neutrality by 2050 through abandoning fossil fuel sources of energy. One of the alternatives is wind energy which accounted for 24% of the UK's energy generation in 2020 and is planned to reach a 50 GW capacity by 2030 [3]. The size and height of wind turbines are increasing to maximise generated power per occupied surface area, which in turn result in strong wakes extending tens of kilometres downwind [7]. Such wakes have the potential risk of reducing downwind farms efficiency [2, 5]. Meso-scale simulations are performed using the Weather Research and Forecasting (WRF) model [9] to understand the large-scale effects of wind farms on neighbouring wind farms by modelling wind turbines as sinks of momentum and sources of turbulence.

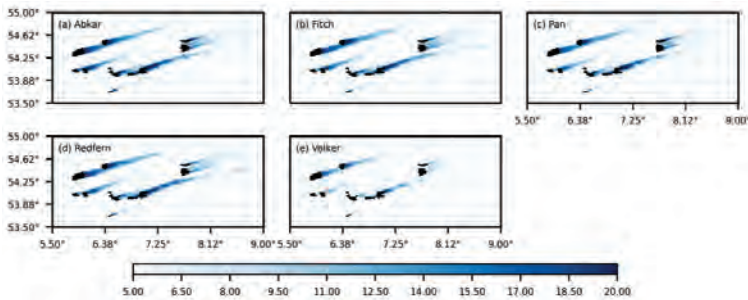
## Setup

Five wind farm parameterisations [1, 4, 6, 8, 10] are implemented in WRF v4.3.3 to simulate 24 physical hours around the shown wind farms, starting from the midnight of October 14<sup>th</sup>, 2017 with the ERA5 re-analysis providing boundary and initial conditions.



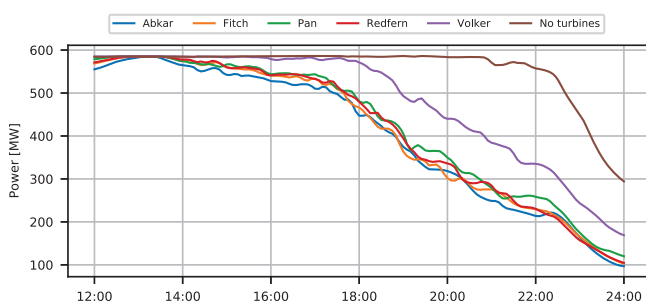
## Wake extent

Shown are contours of normalised wind speed deficit in reference to a case with no wind turbines at 15:00 on October 14<sup>th</sup>, 2017 and at 90 m above the surface. Contours are capped at a minimum of 5% marking a fully recovered wake. Fitch's wake is approximately double that of Volker for the Gode Wind 1 & 2 farms with the former extending 110 km downwind.



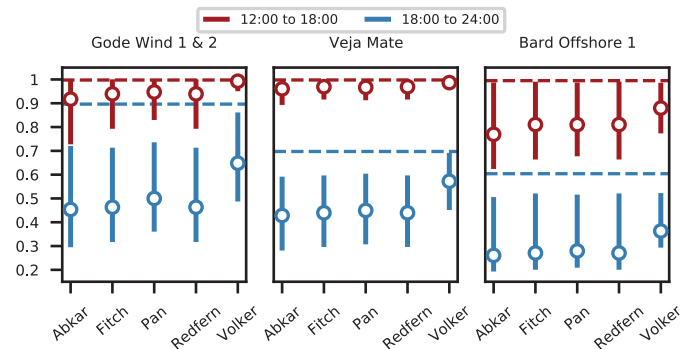
## Power generation of Gode Wind 1 & 2

The time evolution of generated power from the Gode Wind 1 & 2 farms, whose rated power is 600 MW, shows that from 18:00 onward, Volker's power generation is on average 40% higher than the others due to weaker wakes and less momentum extraction by the wind turbines.



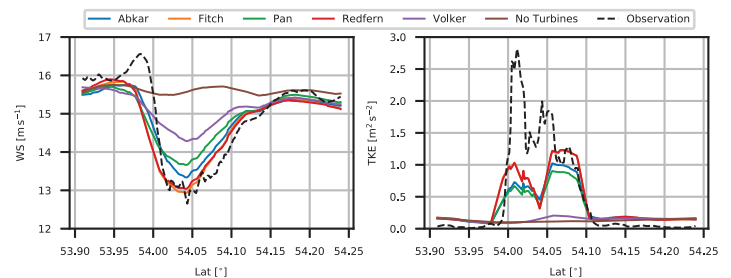
## Capacity factor (actual power in reference to rated power)

Minimum, maximum, and average capacity factor for three wind farms with rated powers of 600, 402, and 400 MW, respectively. Dashed lines represent an upper threshold of capacity factor in case of no wind turbines. When the wind turbines of Veja Mate are removed, the capacity factor of Bard Offshore 1 rises from 0.82 to 0.95 using Fitch's parameterisation.



## Transect flight over Gode Wind 1 & 2

Comparing simulated wind speed and TKE to the airborne measurements [7] over the Gode Wind 1 & 2 farms at a height of 250 m shows that Fitch's and Redfern's parameterisations are the closest to measurements.



## Conclusions

- ▶ Volker's parameterisation predicts shorter wakes, higher power generation, and much less TKE than the other parameterisations.
- ▶ Wake lengths using Volker's parameterisation are approximately half of that of Fitch's parameterisation.
- ▶ Inter-array wake effects can be significant if wind farms are in close proximity like in the case of Veja Mate and Bard Offshore 1 where the latter loses around 52 MW when operating at rated wind speeds.

## References

- [1] Mahdi Abkar and Fernando Porté-Agel. *Journal of Renewable and Sustainable Energy*, 7(1):013121, 2015.
- [2] Naveed Akhtar and et al. *Scientific Reports*, 11(1):17578, Aug 2021.
- [3] Department for Business, Energy & Industrial Strategy. Energy white paper: Powering our net zero future, Dec 2020.
- [4] Anna C. Fitch and et al. *Monthly Weather Review*, 140(9):3017 – 3038, 2012.
- [5] J. K. Lundquist and et al. *Nature Energy*, 4(1):26–34, Jan 2019.
- [6] Yang Pan and Cristina L. Archer. *Boundary-Layer Meteorology*, 168(3):469–495, Sep 2018.
- [7] Andreas Platis and et al. *Scientific Reports*, 8(1):2163, Feb 2018.
- [8] Stephanie Redfern and et al. *Monthly Weather Review*, 147(3):1029 – 1046, 2019.
- [9] William C. Skamarock and et al. UCAR/NCAR, 2019.
- [10] P. J. H. Volker and et al. *Geoscientific Model Development*, 8(11):3715–3731, 2015.

**Acknowledgements** The authors would like to acknowledge the assistance given by Research IT and the use of the Computational Shared Facility at The University of Manchester.

# Wind farm parameterisation in WRF

Karim Ali <sup>a</sup>, Timothy Stallard <sup>a</sup>, David M. Schultz <sup>b,c</sup>, Alistair Revell <sup>a</sup>, and Pablo Ouro <sup>a,b</sup>

<sup>a</sup> School of Engineering, University of Manchester, UK

<sup>b</sup> Centre for Crisis Studies & Mitigation, University of Manchester, UK

<sup>c</sup> Centre for Atmospheric Science, Department of Earth & Environmental Sciences, University of Manchester, UK

The United Kingdom (UK) is aiming at achieving carbon neutrality by 2050 through abandoning fossil fuel sources of energy. One of the alternatives is wind energy which accounted for 24% of the UK's energy generation in 2020 and is planned to reach a 50 GW capacity by 2030 [3]. The size and height of wind turbines are increasing to maximise generated power per occupied surface area, which in turn result in strong wakes extending tens of kilometres downwind [7]. Such wakes have the potential risk of reducing harvesting efficiency of downwind farms and wasting future wind resource [2, 5]. Meso-scale simulations are performed to understand the large-scale effects of wind farms on neighbouring wind farms by modelling wind turbines as sinks of momentum and sources of turbulence. The Weather Research and Forecasting (WRF) model [9] is used in this study to contrast five wind farm parameterisations [1, 4, 6, 8, 10] through simulating multiple wind farms in the North Sea region using the ERA5 re-analysis for boundary and initial conditions.

Through comparison to airborne measurements, Volker's parameterisation underestimates turbulence as well as a wind farm's wind speed deficit leading to an average of 40% higher prediction of power generation than the other parameterisations. Its resulting wakes are approximately half of that predicted by Fitch's parameterisation which extends 110 km downwind of the Gode Wind 1 & 2 farms. Inter-array wake effects can be significant if wind farms are in close proximity like in the case of Veja Mate and Bard Offshore 1 where the latter loses around 52 MW when operating at rated wind speeds due to the former's wakes. Within the current study, the corrections to Fitch's parameterisation introduced in Redfern's parameterisation result in insignificant differences. Also, at fine horizontal grid resolution, Pan's parameterisation is close to that of Fitch. The two parameterisations can deviate in case coarser meshes are used.

## References:

- [1] Mahdi Abkar and Fernando Porte-Agel. *Journal of Renewable and Sustainable Energy*, 7(1):013121, 2015.
- [2] Naveed Akhtar et al. *Scientific Reports*, 11(1):17578, Aug 2021.
- [3] Department for Business, Energy & Industrial Strategy. *Energy white paper: Powering our net zero future*, Dec 2020.
- [4] Anna C. Fitch et al. *Monthly Weather Review*, 140(9):3017 – 3038, 2012.
- [5] J. K. Lundquist et al. *Nature Energy*, 4(1):26–34, Jan 2019.
- [6] Yang Pan and Cristina L. Archer. *Boundary-Layer Meteorology*, 168(3):469–495, Sep 2018.
- [7] Andreas Platis et al. *Scientific Reports*, 8(1):2163, Feb 2018.
- [8] Stephanie Redfern et al. *Monthly Weather Review*, 147(3):1029 – 1046, 2019.
- [9] William C. Skamarock et al. *UCAR/NCAR*, 2019.
- [10] P. J. H. Volker et al. *Geoscientific Model Development*, 8(11):3715–3731, 2015.

## The X-Rotor concept

The X-Rotor is an X-shaped vertical axis wind turbine that employs secondary rotors for power take off. The primary rotor design increases the swept area of the primary rotor whilst mitigating the overturning moments associated with rotors in a V configuration. Additionally, the lower blades provide the attachment location for the secondary rotors.

The primary rotor is allowed to spin freely on its axis and the rotor speed is controlled through upper blade pitch actuation and the thrust on the secondary rotors. All power take off is completed through the secondary rotors.



## Benefits of secondary rotors

Due to the high apparent windspeed on the secondary rotors, they require only a small swept area to provide the rated power, allowing the secondary rotors to rotate 50 times faster than the primary rotor. This facilitates the use of direct drivetrains without using large multipole generators, significantly reducing the size and weight on the drive train when compared to traditional designs. The smaller generators lead to a significantly reduced capital cost (up to 32%[1]) whilst the combination of the lightweight generator and the near-ocean-surface location of the secondary rotor module result in significantly reduced operations and maintenance costs (up to 55%[1]).

## Physics of secondary rotors

There are two key principles to understand about secondary rotors, these are:

1. For steady operation, the aerodynamic torque on the primary rotor must be matched by the torque generated by the aerodynamic thrust on the secondary rotors.
2. The efficiency of power conversion between the primary and secondary rotors is dictated by the ratio of the secondary rotor power coefficient to thrust coefficient.

The first principle allows us to derive the operational thrust coefficient of the secondary rotor, whilst the second informs us that the operational thrust coefficient should be minimised in order to maximise the conversion efficiency.

## Secondary rotor design

The secondary rotor is designed such that its operational thrust coefficient provides the counter torque required to operate the primary rotor in maximum power point tracking. BEM based optimal rotor design theory[2] is employed to determine the rotor design that maximises the secondary rotor power coefficient.

The design is constrained both by the maximum tip speed limits and by the minimum allowable rotational speed at rated power. The efficiency of energy conversion is maximised as the secondary rotor thrust coefficient is minimised, thus the optimal secondary rotor is designed to operate at the minimum allowable rotational speed so as to maximise its area under tip speed constraints thus minimising the operational thrust coefficient.

## How can we create a parametric model to explore the design space?

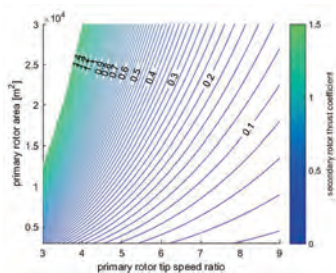
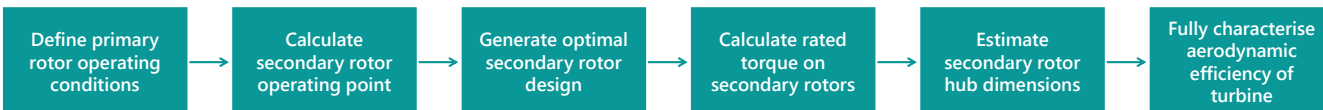


Figure 1: Secondary rotor design thrust coefficient for a range of primary rotor configurations.

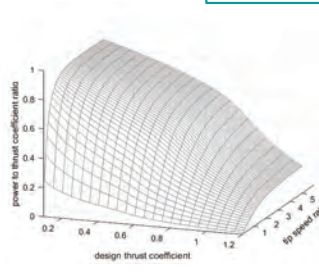


Figure 2: Ratio of power to thrust coefficient for a range of optimally designed 5 bladed rotors.

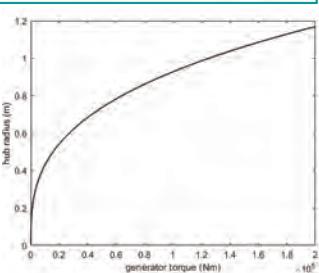


Figure 3: The relationship between generator torque and hub radius assuming similarity scaling.

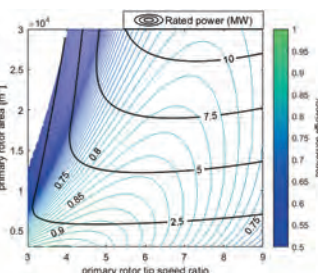


Figure 4: Exemplar contour plot of conversion efficiency between the primary and secondary rotor.

## Exploring upscaling using secondary rotors

Figure 5 shows exemplar outputs from the parametric X-Rotor design tool with an assumed primary rotor power coefficient of 0.45 (shown to be achievable in [3]), a rated windspeed of 12m/s, and a 25Hz constraint on the electrical frequency into the power converters. These results demonstrate how secondary rotors provide a scalable power take off solution with high rated powers becoming available as more secondary rotors are employed.

Conversion efficiencies of 0.86 are achievable for 5MW, 7.5MW, 10MW and 15MW designs, with 2, 3, 4 and 6 secondary rotors respectively. This leads to effective power coefficients of 0.39. Whilst this is considerably lower than the values achievable by high performance horizontal axis wind turbines, the considerable cost reductions associated have previously demonstrated that the X-Rotor concept can provide a significant reduction in the cost of energy. Work on full cost of energy estimates is ongoing as part of the X-Rotor H2020 project.

## References

- [1] Leithead, W., Camciuc, A., Amiri, A. K., & Carroll, J. (2019). The X-Rotor Offshore Wind Turbine Concept. *Journal of Physics: Conference Series*, 1356(1), 0-10.
- [2] Jamieson, P. (2018). *Innovation in wind turbine design* (2nd ed.). Wiley
- [3] Morgan, L., & Leithead, W. (2022). Aerodynamic Modelling of a Novel Vertical Axis Wind Turbine Concept. *Journal of Physics: Conference Series*, 2257(1), 012001.

## Acknowledgements

The authors would like to acknowledge the EU H2020 XROTOR Project 101007135, and the EP/S023801/1 EPSRC Centre for Doctoral Training in Wind and Marine Energy Systems and Structures for funding this research.

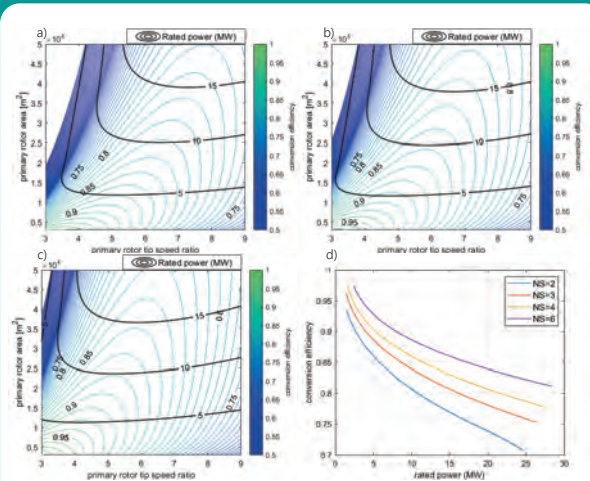


Figure 5: Power coefficient contours alongside turbine rated power contours for a range of primary rotor configurations with optimally designed secondary rotors with the number of secondary rotors 3, 4 and 6 secondary rotors employed in sub figures a), b), c). Subfigure d) shows the conversion efficiency as rated power increases for the cases considered here.

## **Exploring the use of secondary rotors for vertical axis wind turbine power take off.**

Laurence Morgan – University of Strathclyde

Offshore wind energy is set to play a key role in the decarbonisation of the global energy system. Whilst the offshore wind sector has been successful, deployment of new capacity must be significantly increased to limit warming to 1.5 degrees in accordance with the Paris agreement. Decreasing the cost of energy is an effective method to accelerate the deployment of offshore wind. This can typically be achieved through either incremental innovation or radical innovation. This work focuses on the latter, exploring the use of secondary tip rotors to provide wind turbine power take-off.

Traditionally wind turbine power take-off is completed through an electrical machine connected to the rotor shaft either directly or through a gearbox as a sub-system referred to as the drivetrain. Due to the low rotational speed of the wind turbine rotor, the input torque is typically very high leading to heavy, expensive drivetrains. Additionally, as these drivetrains are located at the rotor hub height (typically in excess of 100m above sea level), the operations and maintenance costs associated with the drivetrain are also large. Whilst vertical axis wind turbines can utilise drivetrains located at the base of the turbine, the inherently low rotational speeds and large aerodynamic torque ripple lead to expensive drivetrains that can be prone to failure.

Secondary rotors attached to a turbine's blade tips can provide an alternative means of power take-off. They experience an average inflow velocity equal to the product of the primary rotor tip speed ratio and the inflow wind speed, thus for a typical vertical axis wind turbine, the secondary rotors experience a kinetic energy flux approximately 125 times higher than the primary rotor. This allows them to be significantly smaller whilst providing an equivalent power output. Due to their small radius, the secondary rotors can rotate at a significantly increased speed, leading to a drivetrain torque approximately 65 times lower than that experienced by an equivalent horizontal axis turbine. This high-speed drivetrain also allows the use of direct drive drivetrains without large multipole generators, leading to significantly lower capital costs. Additionally, the near-ocean-surface location of the secondary rotors lowers the estimated operations and maintenance costs significantly.

This poster introduces the X-Rotor concept and describes the development of a parametric model to derive the coupled aerodynamic efficiency of vertical axis wind turbine systems that utilise secondary rotors for power take-off. This method is based on a characterisation of the dynamics of the coupled primary and secondary rotors, then utilises an extension of BEM-based optimal rotor design theory to evaluate the maximum achievable performance of the secondary rotors. The effects of the secondary rotor hub on aerodynamic performance are included through an iterative scheme coupling the rated power of the turbine drivetrain to the hub diameter. The scalability of secondary rotors is explored by increasing the number of secondary rotors employed.

# Investigation into the Coupling of a Wave Energy Converter with a Reverse Osmosis Desalination Plant

Tapas K. Das, Matt Folley, Carwyn Frost  
Queen's University Belfast

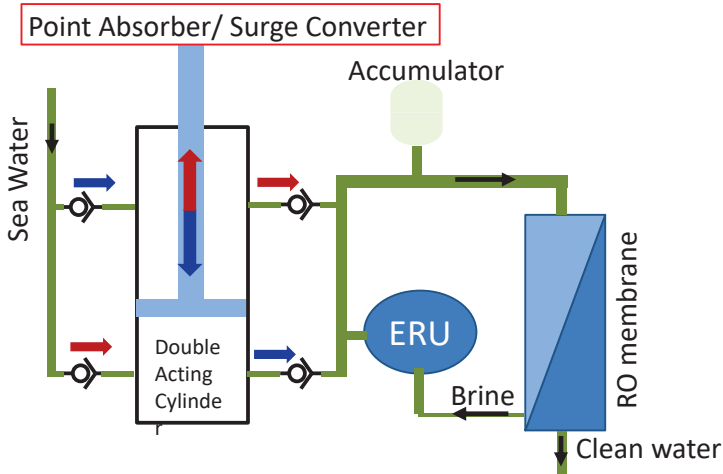
## Introduction

Direct coupling to the hydraulic output of a wave energy converter (WEC) to a desalination plant poses several challenges the most significant being that reverse-osmosis (RO) plant does not normally operate in variable inflow conditions. This research investigates the direct coupling of wave energy converters to reverse osmosis desalination plant powered by pressurized water from the primary power take off system.

## Project Activities

- Review of WEC PTO suitability and characteristics
- Commissioning of RO laboratory test rig
- Laboratory test programme
- Numerical modelling of wave-powered desalination systems
- Design guidelines for wave-powered desalination

## A Wave Powered Desalination Plant



## Desalination Experiment Rig

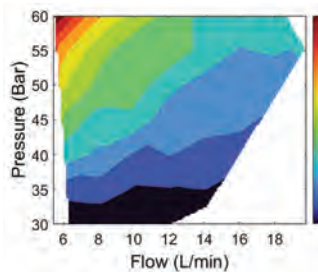
### Reverse Osmosis Module



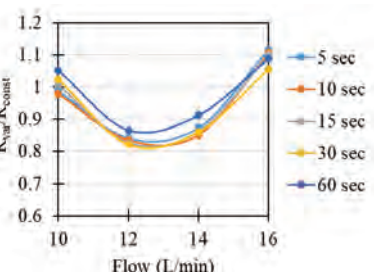
High Pressure Pump Accumulator Water Tank

## Laboratory Test Programme

- Constant flow and pressure
- Constant flow and variable pressure
- Variable flow and constant pressure

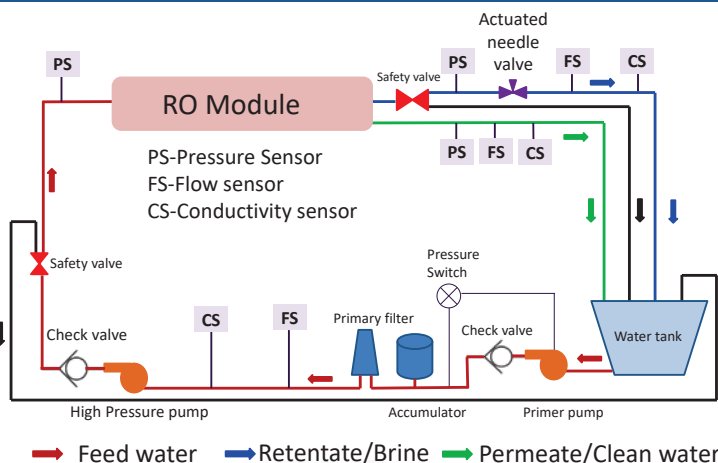


Permeate recovery for constant flow & pressure



Ratio of permeate recovery for variable pressure to constant pressure

## Schematic of Experimental Setup



➔ Feed water ➔ Retentate/Brine ➔ Permeate/Clean water

## Project Outcome

- Develop understanding
  - ❑ Understanding physical processes taking place in reverse osmosis plant
  - ❑ Correlation between the numerical and physical predictions
  - ❑ Investigate the design of wave powered desalination with or without flow conditioners such as accumulator
- Stimulate interest in deploying WEC technology for desalination
- Create a road map for wave-powered desalination



# Investigation into the Coupling of a Wave Energy Converter with a Reverse Osmosis Desalination Plant

Tapas K. Das, Matt Folley, Carwyn Frost  
Queen's University Belfast, Northern Ireland

## Abstract:

The present research focuses on the direct coupling of wave energy converters to reverse osmosis desalination plant powered by pressurised water from the primary power take off system. Although reverse-osmosis desalination plant driven by renewable energy currently exists, they have mostly used an electric pump to provide a relatively stable saline water flow. Direct coupling to the hydraulic output of a WEC poses several challenges the most significant being that reverse-osmosis (RO) plant does not normally operate in variable inflow conditions and consequently there is very little published research in this area. As not all WEC concepts are suitable for direct hydraulic coupling to RO plant, it is essential to develop a target specification and apply it to current and proposed technology. The poster will present the development strategies of an experimental setup of a wave powered desalination plant.

# Unsteady Loading Tidal Turbine Benchmarking Study

Dr. S.T. Harvey<sup>1</sup>, Dr. X. Chen<sup>1</sup>, Prof. R. Willden<sup>1</sup>, Dr. K. Bhavsar<sup>2</sup>, Dr. T. Allsop<sup>2</sup>, Prof. J. Gilbert<sup>2</sup>  
 Dr. H. Mullings<sup>3</sup>, Prof. T. Stallard<sup>3</sup>, I. Benson<sup>4</sup> and Dr. A. Young<sup>4</sup>

<sup>1</sup> University of Oxford, <sup>2</sup> University of Hull, <sup>3</sup> University of Manchester, <sup>4</sup> University of Bath



UNIVERSITY OF OXFORD



Offshore Renewable Energy



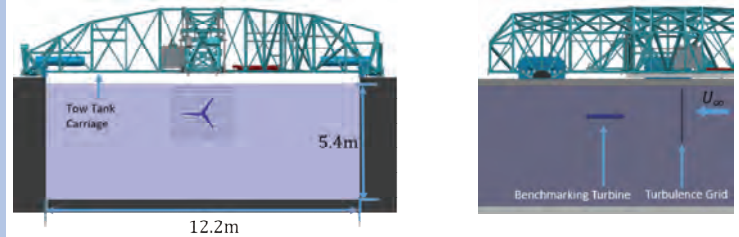
Engineering and Physical Sciences Research Council

## Motivation

- Unsteady loading and the inability to confidently predict unsteady loading and / or quantify errors drives unnecessary **redundancy and design conservatism**.
- The objectives of proposing this tidal turbine benchmarking exercise is to:
  - improve accuracy of modelling techniques
  - improve confidence in the use of modelling techniques
  - quantify modelling errors for different techniques under different loading scenarios
  - development of novel measurement techniques
- The approach that we proposed to achieve the targets:
  - Conduct a large laboratory test of a highly instrumented tidal turbine in **turbulent flow and waves** to provide underlying data
  - Conduct a series of community wide (academia and industry) **blind prediction exercises** with staged data release, leading to an open access dataset
- This project is funded jointly by EPSRC Fellowship EP/R007322/1 and the EPSRC Supergen ORE HUB EP/S000747/1

## Testing Facility and Turbulence Generation

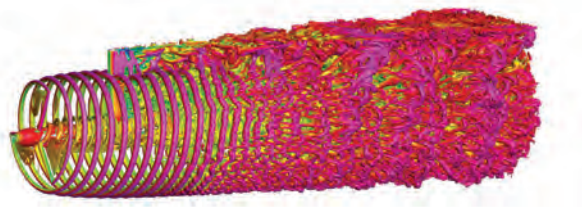
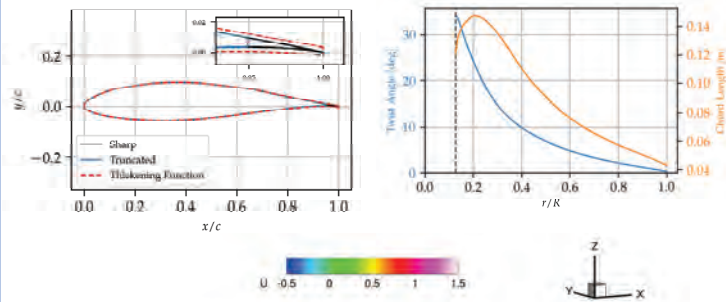
- Tests conducted in QinetiQ towing tank in Portsmouth
- Large cross-section of tank provides a low blockage of **3.05%**
- A 2.4 × 2.4m **carriage-mounted** turbulence grid is used to elevate the turbulence level for the turbulent test case



## Turbine Design and Instrumentation

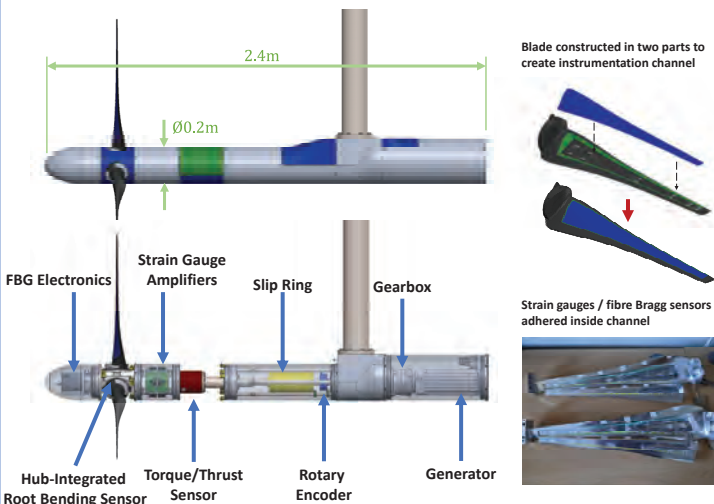
### Blade Design and Modelling

- The benchmarking turbine is designed using RANS-BE CFD simulations
- A single hydrofoil profile, **NACA 63-415**, is used throughout from hub to tip
- Ratio between the trailing edge thickness and chord length is kept constant
- The design was checked with both blade-resolving and CFD-AL simulations



### Instrumentation

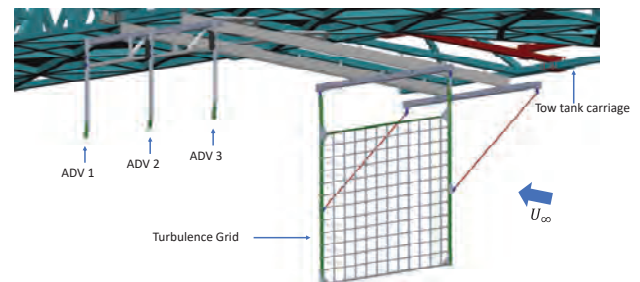
- 2 blades instrumented with strain gauges at 6 radial locations for flapwise and edgewise bending moments, in total over **100** individual strain gauges
- Remaining blade instrumented with fibre Bragg sensors by University of Hull team
- Rotor integrated loads measured by Torque/Thrust transducer



## Experimental Campaigns

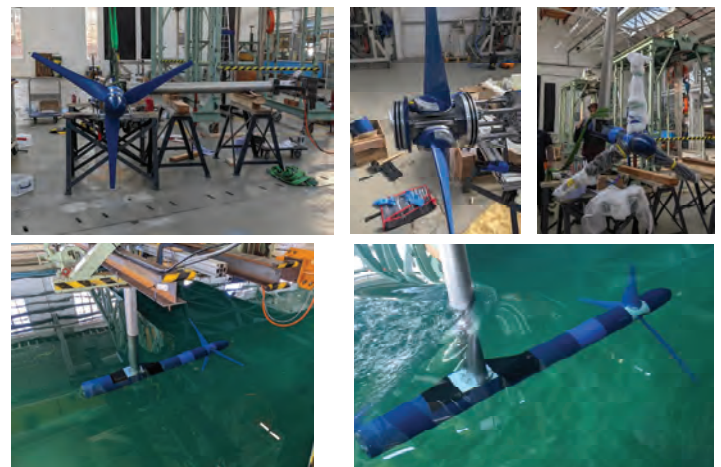
### July 2021: Flow Characterisation

- Flow behind turbulence grid characterised with the use of Acoustic Doppler Velocimeters
- Additional characterisation with Barnicle probe developed by University of Bath team during March 2022 campaign
- Swept-area averaged turbulence intensity of **3.1%** with a streamwise velocity of **0.92U<sub>∞</sub>**



### March 2022: Turbine Testing

- Testing of **steady and elevated turbulence** cases completed
- Some wave testing completed although additional testing to be performed **November 2022**



## Project Participation

- Stage I simulation stage in progress
- 29** active participants from **6** countries
- Large range of modelling methodologies:
  - BEM
  - BEIM
  - Actuator Disk
  - Vortex Panel Methods
  - Actuator Line – RANS/LES
  - Blade Resolved – RANS/URANS/DES
- Project webpage: <https://supergen-ore.net/projects/tidal-turbine-benchmarking>



# Unsteady Loading Tidal Benchmarking Project: Poster Abstract

Sam Tucker Harvey

September 14, 2022

Uncertainty in tidal turbine loading is a major contributor to conservatism in rotor design and hence elevates the levelised cost of energy. This uncertainty originates not only from a lack of knowledge of the flow field at a particular site, but also from lack of understanding of the fundamental physics which govern the loading and performance of tidal turbines in unsteady and turbulent flow regimes. In order to reduce this conservatism and the costs associated, the mathematical and engineering models utilised in turbine design must be improved. To facilitate the development of these models requires scale experimental data for validation. However, few well-documented experimental data sets are available for tidal turbines, especially at scales large enough to achieve Reynolds number independence and comparability to full scale devices.

The tidal turbine benchmarking project has conducted a large laboratory scale experiment on a highly instrumented 1.6 m diameter tidal rotor. The turbine was instrumented for the measurement of spanwise distributions of flapwise and edgewise bending moments and was tested in well-defined flow conditions, including wave generated unsteadiness and freestream turbulence. The turbine was tested in the QinetiQ towing tank facility, based in Portsmouth, to achieve the required incident current and wave conditions with a low blockage of 3.05%.

As towing tank facilities by their nature have very low levels of freestream turbulence, a carriage-mounted turbulence grid has been developed to allow the level of turbulence to be elevated in the experiments. The turbulence grid, which is constructed of aluminium extrusions mounted to a rectangular outer frame, is designed to allow for varying levels of turbulence to be produced by altering the number of bars. Before experiments were performed with the benchmarking turbine behind the turbulence grid, the flow behind the turbulence grid was characterised. This characterisation was performed with the use of an Acoustic Doppler Velocimeters (ADV), in particular the Nortek Vectrino. Velocity measurements were made at a series of cross-stream locations within the intended turbine plane, while seeded water was introduced into the towing tank prior to each set of experimental runs. The variation of the streamwise velocity across the region that will be occupied by the turbine was found to be small, varying within 0.5% of the mean value over this region. The velocity deficit was also found to be small, with a mean value of  $0.92U_\infty$  across the same region, with a corresponding mean streamwise turbulence intensity of 3.1%.

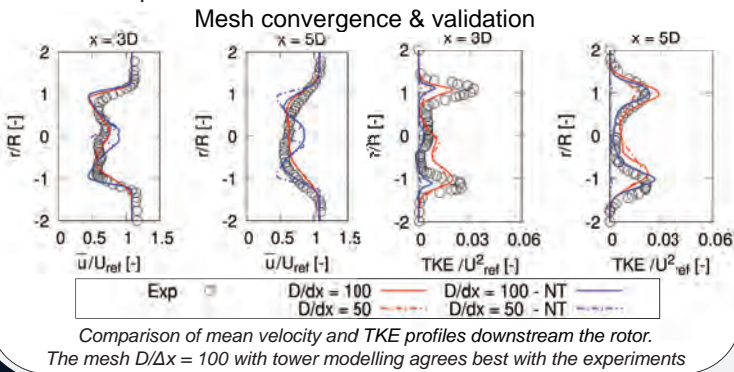
Following the experimental testing, an initial round of blind benchmarking has begun, in which engineers from academia and industry have been invited to predict the loading experienced by the turbine under steady flow and elevated turbulence conditions. The benchmarking rounds and staged release of experimental data will enable engineers to understand the limitations of their models and provide data to enable modelling improvements.

## Introduction

Data decomposition methods are applied in high-fidelity CFD data of wind turbine wakes to better understand the dynamics of these flows. The data decomposition algorithms can reveal non-trivial coherent structures that are responsible for the behaviour of those complex flows. They can also provide a low dimensionality basis that can be used to build reduced order models for the prediction of those flows.

## Numerical Methods

- Rotor: NTNU Blind Test 1 [1],  $D = 1m, TSR = 6, U_\infty = 10 m/s$ .
- CFD Solver: LES with Smagorinsky,  $C_s = 0.21$ .
- Turbine representation: Actuator Line Method [2].
- Tower: VoF type method [3].
- Mesh size: 20M ( $D/\Delta x = 100$ ).
- Time step:  $T/\Delta t = 100$ .



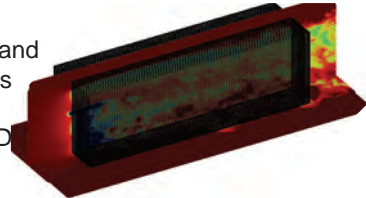
## High Order Dynamic Mode Decomposition

- First introduced by LeClairche and Vega (2017) [4] as an extension to the classic DMD algorithm that decomposes a flow into:

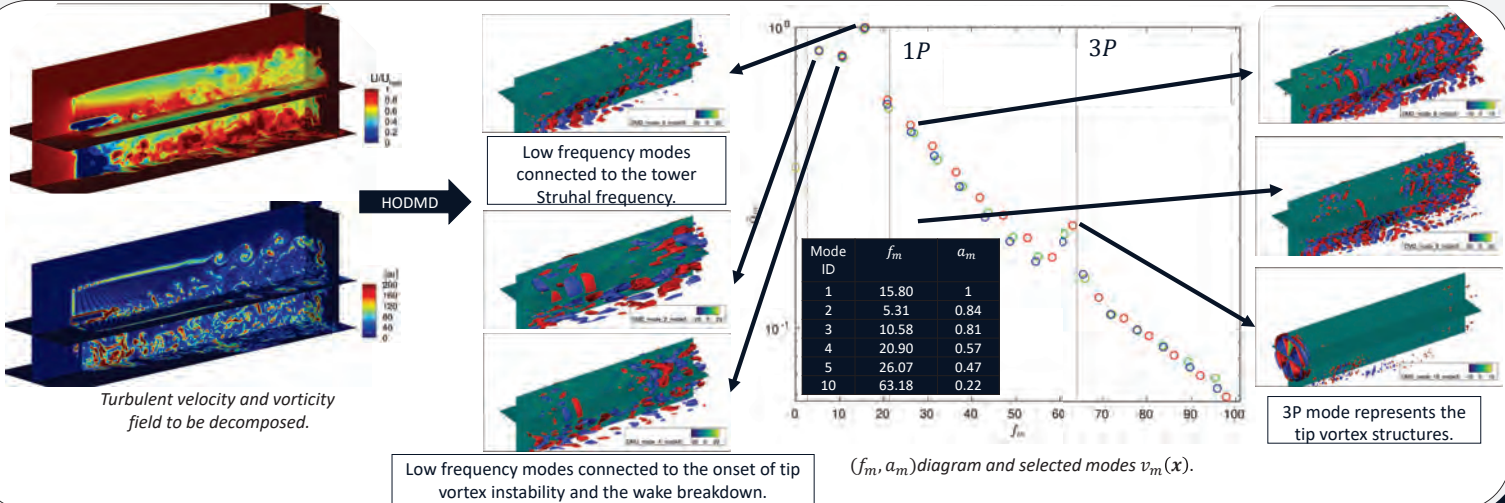
$$X_k^{DMD} = \sum_{m=1}^M a_m v_m(x) e^{(\delta_m + i\omega_m)(k-1)\Delta t}, k = 1, \dots, K$$

Labels: Spatial structure, Mode  $m, v_m(x)$ , Temporal evolution, Fluctuating Flow Field  $u'(x, t)$ , Scalar amplitude of mode  $m$ , Growth Rate, Frequency

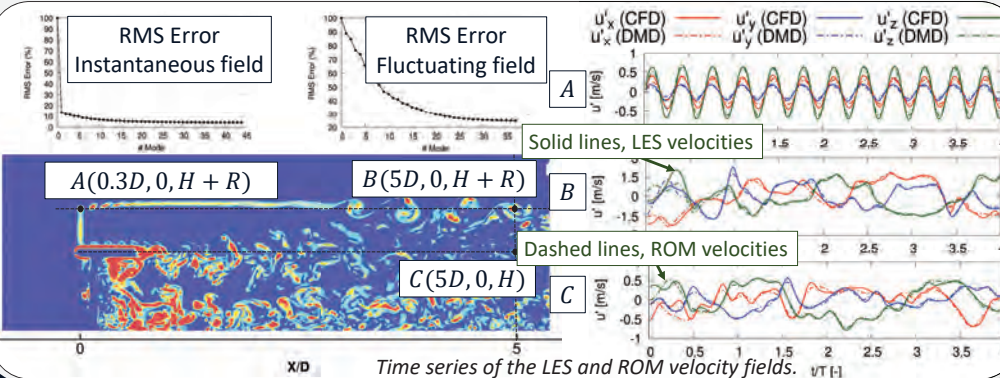
- The HODMD adds robustness and flexibility to the classic DMD thanks to the time-delay theorem.
- The data used to apply HODMD are interpolated from the LES simulation, in a coarser mesh,  $D/\Delta x=50$  and time-step  $T/\Delta t = 50$ .



## Modal decomposition



## Reduced order model



## Conclusions

- The wake of a wind turbine was decomposed into **37 modes**, the most dominant of which are in low frequencies and correspond to the **tower shedding and wake breakdown**.
- **1P and lower frequencies** are connected to the **onset of the tip vortex mutual inductance instability and the wake breakdown**.
- The characteristic **3P frequencies**, rank **10<sup>th</sup>** in terms of reconstruction error and are connected to the tip vortices.
- A reduced order model is built that reconstructs the **overall velocity field with 7% and fluctuating velocity field with 25% error**.

## Dynamic Mode Decomposition of Wind Turbine Wakes

Markella Zormpa<sup>1</sup>, Soledad Le Clainche<sup>2</sup>, Esteban Ferrer<sup>2</sup>, Christopher Vogel<sup>1</sup>, Richard Willden<sup>1</sup>

<sup>1</sup>Department of Engineering Science, University of Oxford

<sup>2</sup>School of Aeronautics, Universidad Politécnica de Madrid

Moving away from carbon-intensive energy generation methods will require a drastic increase in the uptake of large wind farm installations. In fact, the UK has committed to installing 50GW of offshore wind energy by 2030 [1], almost quadrupling the current 12.7 GW installed capacity [2]. Large offshore wind farms suffer from power losses mostly related to the wake effect that can cause a 10 - 20% decrease in overall farm power production [3]. It is therefore necessary to understand and model the wakes of wind turbines, in order to better predict and control power production, fatigue loads and other operational aspects of those installations.

Acquiring measurements for the turbulent wake flows, is not a trivial task. 3D experimental data exist for very limited set of operating and environmental conditions due to the inherent difficulties in measuring these flows. Alternatively, turbulent velocity fields, rich in non-linear dynamics, can be calculated using high fidelity large eddy simulations (LES), which is the approach employed in this work. The wind turbine rotors are parameterized using the actuator line method (ALM), and the tower is modelled using a volume of fluid type approach. The simulations are validated against experimental data for a 1m diameter rotor.

The 3-dimensional velocity fluctuations extracted from the LES, are processed using the high order dynamic mode decomposition (HODMD) algorithm [4], a variant of the well-known dynamic mode decomposition (DMD), used in the past decade to analyse, among other problems, turbulent flows. These methods, are capable of decomposing a flow field into coherent structures with a single frequency content and a corresponding amplitude that ranks the flow features in order of relevance for the reconstruction of the flow. The coherent structures as well as the frequency information allow to identify which physics are relatively more important in a flow over other. The dynamic mode decomposition also provides an optimal basis, on which the flow can be modelled with significantly reduced dimensionality than the original representation, creating a reduced order model.

In this work, 3-dimensional temporal wake data of a 1m diameter, the NTNU Blind Test wind turbine [5] are produced using LES and are subsequently processed using HODMD. The results reveal non-trivial dynamic modes at frequencies much lower than the blade passing frequency, that have to do with the mutual inductance instabilities and subsequent breakdown of the wake, as well as the tower vortex shedding. Near and far-wake modes are identified at high and low frequencies respectively. A reduced order model is constructed, proving that the flow can be reconstructed with low error in the time domain, using only 37 modes.

[1] <https://www.gov.uk/government/news/major-acceleration-of-homegrown-power-in-britains-plan-for-greater-energy-independence>. Accessed September 2022.

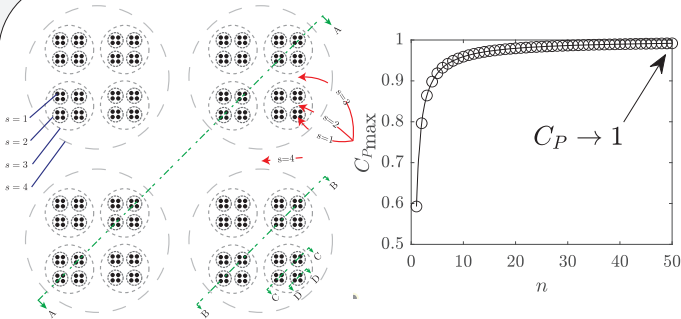
[2] <https://www.renewableuk.com/page/UKWEDhome/Wind-Energy-Statistics.htm>. Accessed September 2022.

[3] Barthelmie RJ, Hansen KS, Frandsen ST, et al. Modelling and measuring flow and wind turbine wakes in large wind farms offshore. *Wind Energy*:12:431-444, 2009.

[4] Le Clainche, S. & Vega, J. M. Higher Order Dynamic Mode Decomposition. *SIAM J. Appl. Dyn. Sys.* 16(2):882–925, 2017.

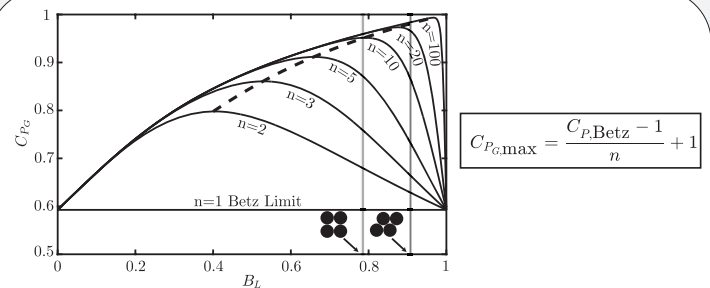
[5] Krogstad, P. & Eriksen, P. "Blind test" calculations of the performance and wake development for a model wind turbine. *Renewable Energy* 50:325-333, 2013.

## Introduction



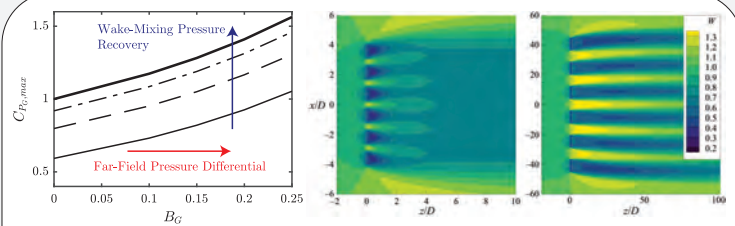
- The limit of energy extraction from an unconstrained flow is 16/27 of the upstream kinetic flux contained by the energy extractor area, known as the “Betz Limit”
- We theoretically [1] demonstrate that by constraining the flow across a range of physical scales we can raise this limit further to a theoretical optima of 100%
- Top left figure is an example of an arrangement of discs which exceed the Betz limit, here for  $n=4$  physical scales
- We then use the model to hypothesise the physical processes that enable the extraction of power above the Betz limit
- Exploiting the underlying physics may uncover both practical and novel configurations for increases in the energy capture efficiency to pave the way for the next generation of wind and tidal turbines

## How does the Power Coefficient vary with Physical Scales?



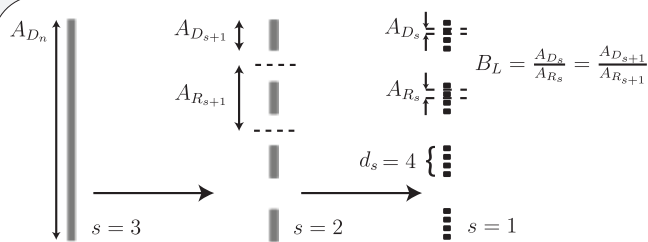
- The maximum power coefficient for a fractal  $n$ -scale device in an infinitely wide channel
- Increases in the number of physical scales raises the maximum power coefficient monotonically
- An analytic expression for the performance of an optimal  $n$ -scale device, where the power coefficient approaches unity in the asymptotic limit is shown

## How is the Power Extraction Efficiency Increased?



- Contrary to intuition, the minimisation of losses is not the mechanism by which the power extraction increases with number of scales
- Wake mixing provides an additional source of static pressure rise in the device wake
- Static pressure on the downstream side of the extractor reduced  $\rightarrow$  increase in the static pressure drop across the device  $\rightarrow$  increased power extraction
- In finite width (tidal) channel, an additional streamwise pressure drop balances device thrust providing an additional basis for increased power extraction
- We additionally demonstrate the performance uplift due to multi-scale dynamics numerically

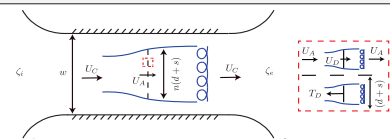
## What are Physical Scales?



- Schematic of a fractal arrangement of turbines
- Recurrent division of discs into  $d$  new sub-discs per division
- Array is split  $n-1=2$  times into  $d=4$  discs each time with constant spacing
- Each additional recurrent division is shown to raise the power extraction efficiency to a limit of 100%

## What is to come?

- We consider the coupling between the channel dynamics [2] and the multi-scale fence theory and develop an analytic model which optimises the number and spacing of turbines in a channel to maximise power per unit turbine area [3]
- We look to exploit the mixing physics to inform next generation turbine design



## Conclusions

- New theoretical upper bound on energy extractor in an unbounded flow (100%). See our paper [1] for more details
- The theoretical model works by constraining the flow across multiple physical “scales” or alternatively the recurrent “splitting” of a turbine
- We show that wake mixing is a key component of the physics underlying this increased energy extraction efficiency
- Equipped with this theoretical understanding, we intend to propose novel flow-constraint based mechanisms to raise the efficiency of next generation turbines

### References

- [1] D. Dehtyriov, A.M. Schnabl, C. R. Vogel, S. Draper, T.A.A. Adcock, R.H.J. Willden. “Fractal-like actuator disc theory for optimal energy extraction”. 2021. *Journal of Fluid Mechanics*, 927:A40.
- [2] C. Garrett, P. Cummins. “The power potential of tidal currents in channels”. 2005. *Proc. R. Soc. A.*, 461:2563-2572
- [3] D. Dehtyriov, C. R. Vogel, R.H.J. Willden. “A head-driven model of turbine fence performance”. Submitted to the *Journal of Fluid Mechanics*.

# Flow Physics Beyond the Betz Limit

Daniel Dehtyriov<sup>1</sup>, Christopher Vogel<sup>1</sup>, Richard Willden<sup>1</sup>

<sup>1</sup> Department of Engineering Science, University of Oxford, Oxford OX1 3PJ, United Kingdom

It has been theoretically shown that tidal fences consisting of multiple turbines placed side-by-side can make use of constructive interference (local blockage) effects to raise the energy extraction efficiency of the fence above that of the Betz limit applicable to unblocked flow problems. For the two-scale problem of a long array of turbines partially spanning the width of a much wider channel (vanishing global blockage) the efficiency of energy extraction, normalised on the undisturbed kinetic energy flux, rises from the Betz limit of 0.593 to the partial fence limit of 0.798 [1]. Experiments on pairs of side-by-side turbines at large laboratory scale [2] have confirmed the important aspects of the underlying partial fence theory and that some of the performance benefits offered by constructive interference effects can be achieved in practice.

Further theoretical work by Cooke et al. [3] showed that if a third scale is introduced to the flow problem, i.e. sub-arrays within the partial fence, that the performance limit can be further increased whilst maintaining negligible global blockage. Theoretical work by Dehtyriov et al. [4] has shown that by adding additional scales to the flow problem, the asymptotic limit on performance of a multi-layered array system is a power coefficient of unity. Further, the performance limit for a given  $n$ -layered system is well approximated by a fractal arrangement of turbines at that scale.

This work further demonstrates that it is not the minimisation of mixing losses by which power extraction increases with the number of scales. On the contrary, wake mixing provides an additional source of static pressure rise in the device wake that enables additional reduction in static pressure on the downstream side of the extractor, and consequently an increase in the static pressure drop across the device, leading to increased power extraction. This performance uplift due to the multi-scale dynamics is additionally demonstrated numerically.

Building on prior work [5] [6], Dehtyriov et al. [7] has further extended the multi-scale fence theory by analytic coupling to the channel dynamics model of Garret and Cummins [8], in which the turbine fences resist the flow rate to the channel. The coupled framework allows for the optimisation of the number (global blockage) and spacing (local blockage) of turbines in a channel to maximise power per unit turbine area as a proxy for revenue vs. cost. Further extensions to the theory will consider proposing novel flow-constraint-based mechanisms to raise the efficiency of next-generation turbines.

## References

- [1] Nishino, T. & Willden, R. H. J. (2012). The efficiency of an array of tidal turbines partially blocking a wide channel. *Journal of Fluid Mechanics*, **708**, 596–606.
- [2] McNaughton, J., Cao, B., Nambiar, A., Davey, T., Vogel, C. R., Willden, R. H. J. (2022). Constructive interference effects for tidal turbine arrays. *Journal of Fluid Mechanics*, **943**, A38
- [3] Cooke, S. C., Willden, R. H. J., Byrne, B. W. (2016). The potential of cross-stream aligned sub-arrays to increase tidal turbine efficiency. *Renewable Energy*, **97**, 284-292.
- [4] Dehtyriov, D., Schnabl, A. M., Vogel, C. R., Draper, S., Adcock, T. A. A., Willden, R. H. J. Fractal-like actuator disk theory for optimal energy extraction. *Journal of Fluid Mechanics*, **927**, A40
- [5] Willden, R. H. J., Nishino, T., Schluntz, J. (2014). Tidal stream energy: designing for blockage. *Proc. 3<sup>rd</sup> Oxford Tidal energy workshop, Oxford, United Kingdom*.
- [6] Muchala, S. Willden, R. H. J. (2017). Impact of tidal turbine support structures on realizable turbine farm power. *Renewable Energy*, **114**, 558-599
- [7] Dehtyriov, D., Vogel, C. R., Willden, R. H. J. A head-driven model of turbine fence performance. Submitted to the *Journal of Fluid Mechanics*.
- [8] C. Garrett, P. Cummins. (2005). "The power potential of tidal currents in channels". *Proc. R. Soc. A.*, **461**, 2563-2572

# Implementing HARM in a 1D Winkler Model to Predict Monopile Response to Cyclic Loading

Jamie Crispin, Harvey Burd & Byron Byrne  
 Department of Engineering Science, University of Oxford  
 jamie.crispin@eng.ox.ac.uk



## (1) Offshore Monopile Foundations

Wind and waves contribute significant horizontal loads over the lifetime of an offshore wind turbine. The foundations, often large diameter monopiles, must be designed to limit deflections to prevent damage.

Load cases such as individual storms, or cumulative effects over the structures entire lifetime must be considered. These can be modelled as time histories, or idealised as sinusoidal packets at different amplitudes. Predicting the foundation response requires an appropriate model to describe the cyclic loading behaviour of the soil.

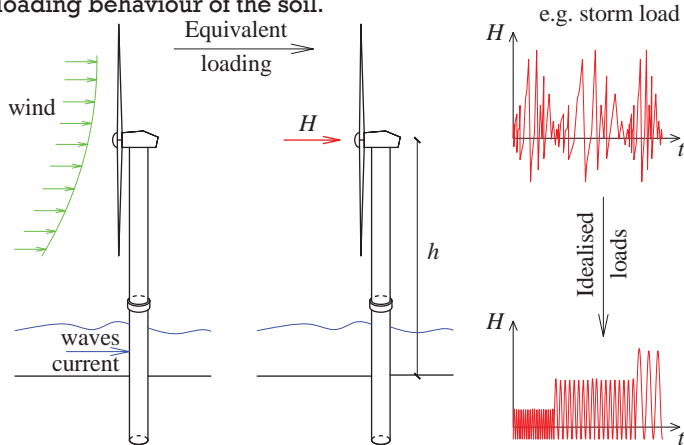


Fig. 1: Wind Turbine Loading

## (2) The HARM Model

A recent approach to modelling cyclic loading of soils is the Hyperplastic Accelerated Ratcheting Model (HARM) [1]. HARM was developed from an Iwan model, a set of elastic springs and plastic sliders arranged in series or parallel. This captures hysteresis and post-cyclic monotonic behaviour.

This has been modified to account for the following experimentally observed behaviours:

- stiffness changes (softening/hardening), through functions of work or strain applied to the slider strength
- accumulation of deformation (ratcheting), through a ratcheting slider connected in series to the Iwan model

The model is shown below for a rate independent case. Rate effects can be introducing using dashpots. HARM can be used directly as a 0D macro-element model to describe the foundation response.

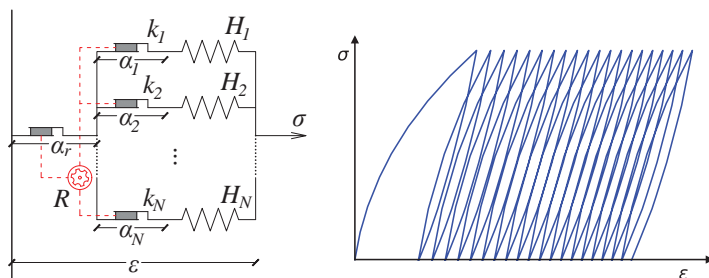


Fig. 2: (a) HARM model configuration [1]; (b) example 0D response

### References:

[1] Houlsby, G.T., Abadie, C.N., W.J.A.P. Beuckelaers & Byrne, B.W. (2017) A model for nonlinear ratcheting behaviour. *International Journal of Solids and Structures*, 120, 68-80.  
 [2] Byrne, B.W., Houlsby, G.T., Burd, H.J., Gavin, K.G., Igoe, D.J.P., Jardine, R.J., Martin, C.M., McAdam, R.A., Potts, D.M., Taborda, D.M.G & Zdravkovic, L. (2020) PISA design model for monopiles for offshore wind turbines: applications to a stiff glacial clay till, *Géotechnique*, 70(11), 1030-1047.  
 [3] Balaam, T.D. (2020) *Development and Calibration of Cyclic Loading Models for Monopile Foundations in Clays*. PhD Thesis, University of Oxford, Oxford, UK.  
 [4] Beuckelaers, W.J.A.P (2017) *Numerical Modelling of Laterally Loaded Piles for Offshore Wind Turbines*. PhD Thesis, University of Oxford, Oxford, UK.  
 [5] Beuckelaers, W.J.A.P, Burd, H.J., Houlsby, G.T., McAdam, R.A. & Byrne, B.W. (2022) A generalised Winkler model for the hysteretic and ratcheting behaviour of monopiles in clay. In: *4<sup>th</sup> International Symposium on Frontiers in Offshore Geotechnics*, Austin, Texas, USA, 1263-1272.

## (3) 1D Winkler Model

0D lumped macro-element models don't directly account for soil properties, particular the variation with depth. This makes them hard to calibrate without large-scale experimental data. 3D finite element (FE) models are prohibitively computationally expensive to run for long time histories and multiple pile and soil configurations.

Instead, a simplified 1D Winkler model can be used. These incorporate variable soil properties with depth, are capable of predicting the response along the whole pile length and can be calibrated against experimental data.

The current work employs the PISA modelling approach [2]. Soil response is captured with four soil reaction curves (shown in Fig. 3). These are each implemented as HARM models.

The pile is modelled as a Timoshenko beam, discretised into multiple elements.

Monotonic soil reaction curves are obtained from calibration against 3D FE.

Ratcheting, softening and rate parameters are calibrated from PISA

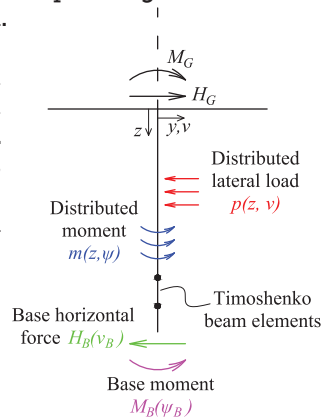


Fig. 3: 1D finite element soil reaction curves [2]

## (4) Modelling PISA CM6

This 1D Winkler approach has been applied to model the response of PISA test pile CM6, installed at a site in Cowden in a glacial clay till. The ground model for the site is given in [2]. Soil reaction curves were based on those in [2], recalibrated for the smaller pile size (see [3-5]). Softening functions, ratcheting functions and rate effects have been calibrated for piles at this site by [3-5]. Result from [3] are used here.

One-way loading was applied in three packets of cycles: 10 at 42.5kN, 10 at 70kN and 38 at 90kN. The modelled behaviour is compared with the measured test results in Fig. 4.

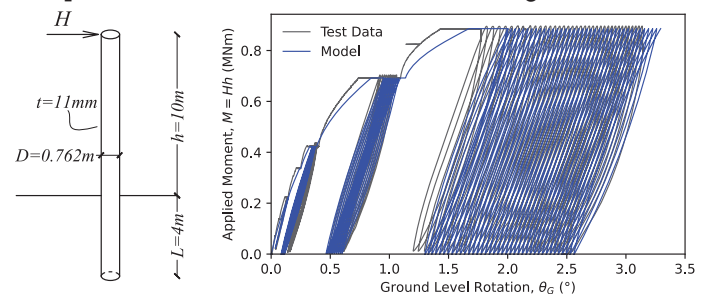


Fig. 4: (a) Pile CM6 dimensions; (b) model response vs. test results Observations:

- Rotations accumulate with cycling (ratcheting), this effect is more pronounced at higher cyclic amplitudes.
- Cyclic stiffness decreases with cycling (softening)
- Properly calibrated, the proposed model can match well with medium scale field test results.

# Title: Implementing HARM in a 1D Winkler model to predict monopile response to cyclic loading

*Jamie Crispin*

**Abstract:** Through both wind and wave loading, offshore wind turbines are subjected to significant horizontal cyclic loading over their design life. These loads are transferred to the foundations, predominantly large diameter monopiles, which must be designed to limit the resulting deflections to prevent damage to the structure. Predicting the foundation response requires an appropriate model to describe the cyclic loading behaviour of soils. One such model is the Hyperplastic Accelerated Ratcheting Model (HARM). It was developed within the hyperplasticity framework from a basic Iwan model, which captures hysteresis and post cyclic monotonic behaviour, that has been modified to also account for stiffness changes (softening/hardening) and accumulated deformations (ratcheting), both of which have been observed experimentally after repeated cycling. Originally employed as a 0D model, HARM can be used directly as a macro-element model to describe the foundation response. However, in this work, a more rigorous 1D Winkler model is employed with the soil reaction curves (e.g. “p-y”) along the pile shaft and at the pile base implemented as HARM models. The resulting model incorporates variable soil properties with depth, is capable of predicting the response along the whole pile length and can be calibrated against experimental data. The modelling approach is applied to an experimental cyclic load test on a monopile installed in a glacial clay till.

# Surface Waves in Open-Channel Flow Over Spanwise Aligned Square Bars

Razieh Jalalabadi, Thorsten Stoesser

Civil, Environmental and Geomatic Engineering, University College London  
r.jalalabadi@ucl.ac.uk

## Introduction

Water surface deformations in open waters are influenced by the sub-surface flow. The underlying flow is also modified by several flow and geometrical parameters such as Froude and Reynolds number and bed roughness topography especially in shallow flows. The objective of this work is to provide better understanding of the effects of underlying flow structure on the generation and dispersion of surface waves

## Methods

- Turbulent open channel flow with two relative submergences over spanwise aligned square bars are simulated using large-eddy simulations.
- For this bar spacing momentum transfer takes place between the area below the crest of the bars and the bulk flow.
- The instantaneous disturbances at the water surface and RMS fluctuations of water surface elevation ( $h$ ) are smaller for Re16000 although Reynolds number is larger in this case (Fig1).

	Re7500	Re16000
$h/k$	2.5	4.25
$Re$	7500	16000
$Fr$	0.46	0.45
$L_x, L_y, L_z$	20.8k, 10.0k, 5.0k	20.8k, 10.0k, 5.0k
$N_x, N_y, N_z$	312, 128, 120	416, 160, 160

Table 1. Hydraulic conditions and computational details.

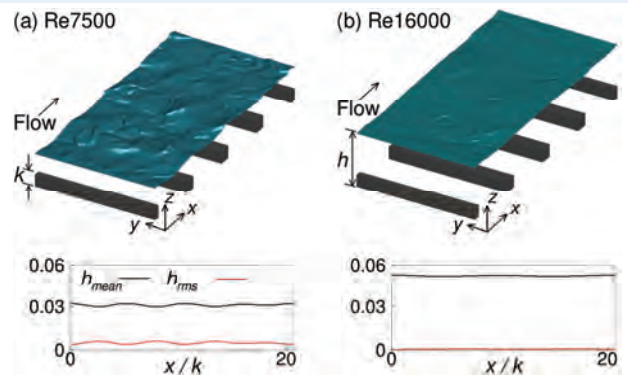


Figure 1. Instantaneous water surface and mean and RMS fluctuations of water surface elevations for (a) Re7500 and (b) Re16000.

## Results

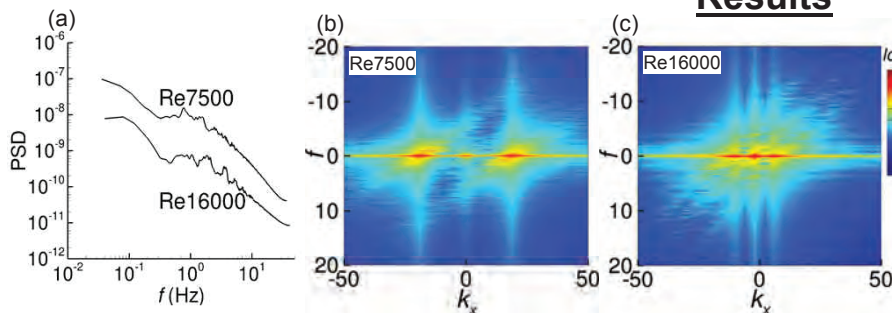


Figure 2. PSD of water surfaces elevation fluctuations (a). Wavenumber-frequency spectra of water surface elevation fluctuations for (b) Re7500 and (c) Re16000.

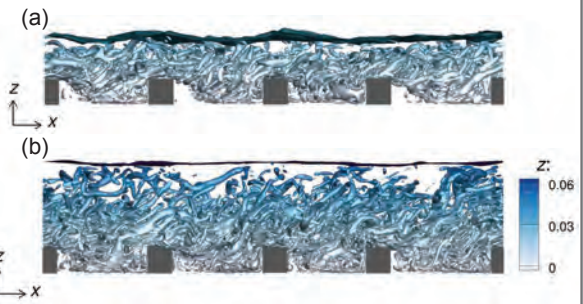


Figure 3. Isosurfaces of  $0.15\lambda_{\alpha, max}$  showing vortical structure for (a) Re7500 and (b) Re16000.

- Dimensional power spectral density (PSD) of  $h'$  in figure 2(a) represents larger energy of the surface waves in Re7500.
- The inclined linear ridges in wavenumber( $k_x$ )-frequency( $f$ ) spectra of  $h'$  in figure 2(b,c) represent convective transport of surface fluctuations with a constant velocity. The inclined central ridge in figure 2(c) corresponds to turbulence induced surface waves which move at the same speed of the flow. Two other ridges at its sides represent waves propagating downstream and upstream. The vertical ridges indicate the stationary waves attributed to the undulations over the water surface induced by the roughness.
- Smaller flow submergence in Re7500 leads to larger interaction of flow and water surface so surface waves energy is larger in this case (figure 3).

## Conclusions

- In flow with smaller submergence there is larger interaction between bulk flow and water surface so the water surface elevation fluctuations and energy of surface waves is larger.
- The surface waves in both cases are either standing waves or transported with a constant phase velocity.
- At higher Reynolds number, turbulent waves are also generated over the water surface which move at the same speed of the flow.

## Acknowledgement

Financial support was provided by the EPSRC/UK project "Rapid Monitoring of River Hydrodynamics and Morphology using Acoustic Holography", grant number EP/R022135/1.

## References

1. R. Jalalabadi, T. Stoesser, P. Ouro, Q. Luo, Z. Xie, J. Hydro-envir. Res., 36, 67 (2021).
2. R. Jalalabadi, T. Stoesser, Phys. Rev. E, 105, 035102 (2022).
3. G. Dolcetti, K. V. Horoshenkov, A. Krynkina, S. Tait, Phys. Fluids, 28, 105105 (2016).

# Surface Waves in Open-Channel Flow Over Spanwise Aligned Square Bars

Razieh Jalalabadi <sup>1\*</sup> and Thorsten Stoesser <sup>1</sup>

<sup>1</sup> Civil, Environmental and Geomatic Engineering, University College London

\*Email: [r.jalalabadi@ucl.ac.uk](mailto:r.jalalabadi@ucl.ac.uk)

Water surface deformations in open waters are influenced by the sub-surface flow. So understanding water surface behavior in free surface flows is crucial as it can be helpful to infer flow conditions under free surface. Although free surface deformations and various types of surface waves have been studied for open channel flows in several works, comprehensive understanding of the effects of underlying bulk flow quantities on the free surface waves are yet to be explored. The underlying flow is modified by several flow and geometrical parameters including Froude ( $Fr$ ) and Reynolds ( $Re$ ) number and channel bed roughness topography as well. Here, we investigate the waves generated over the free surface in a turbulent open channel flow with spanwise aligned square bars as bed roughness. The proposed bar spacing is transitional roughness in which momentum transfer takes place between the area below the crest of the bars and the bulk flow. Two relative submergences which give different Reynolds numbers but similar Froude numbers are considered. The underlying data is generated using large-eddy simulation and free surface elevation is detected using level set method. Table 1 provides hydraulic and computational details for two cases considered.  $H$  is flow depth and  $k$  is bar height. Effects of different flow submergences and Reynolds numbers on the waves generated over the free surface are investigated using spectral analysis. The dimensional power spectral density (PSD) for the fluctuations of free surface elevation are calculated and represent larger energy of the surface waves generated in  $Re7500$  although  $Re$  is smaller in this case. This is attributed to the larger interaction of bars and free surface in  $Re7500$  due to smaller flow submergence in this case. The wavenumber-frequency spectra of free surface elevation fluctuations are calculated to investigate transport mechanism of surface waves. This spectra is calculated using two-dimensional discrete Fourier transform of spatio-temporal correlation of free surface elevation fluctuations in the streamwise direction (Dolcetti *et al.*, 2016). The results generated using this approach reveal that there is convective transport of surface waves propagating downstream and upstream in both flow cases over the free surface while in  $Re16000$  there are also turbulence induced surface waves due to larger  $Re$  which moves at the same speed of the flow. In both cases there are stationary waves that are attributed to the undulations over the free surface induced by the roughness (Jalalabadi *et al.* 2021 Jalalabadi and Stoesser 2022).

Case	$H/k$	$Re$	$Fr$	$L_x, L_y, L_z$	$N_x, N_y, N_z$
<b>Re7500</b>	2.5	7500	0.46	$20.8k, 10.0k, 5.0k$	312, 128, 120
<b>Re16000</b>	4.25	16000	0.45	$20.8k, 10.0k, 5.0k$	416, 160, 160

Table 1. Hydraulic conditions and computational details.  $L_x, L_y, L_z$  are length of the domain in streamwise, spanwise and wall-normal directions and  $N_x, N_y, N_z$  are grid number in these directions.

## Acknowledgments

Financial support was provided by the EPSRC/UK project “Rapid Monitoring of River Hydrodynamics and Morphology using Acoustic Holography,” Grant No. EP/R022135/1.

## References

- Dolcetti, G., Horoshenkov, K. V., Krynkin, A. & Tait, S. J. 2016, Frequency-wavenumber spectrum of the free surface of shallow turbulent flows over a rough boundary, *Phys. Fluids*, **28**, 105105.
- Jalalabadi, R., Stoesser, T., Ouro, P., Luo, Q. & Xie, Z. 2021, Free surface flow over square bars at different Reynolds numbers, *J. Hydro-envir. Res.*, **36**, 67.
- Jalalabadi, R. & Stoesser, T., 2022, Reynolds and dispersive shear stress in free-surface turbulent channel flow over square bars, *Phys. Rev. E*, **105**, 035102.

# A new strategic tool to structure Cumulative Impact Assessment



m.declerck.19@abdn.ac.uk



@Morgane\_Dclrck

Morgane Declerck

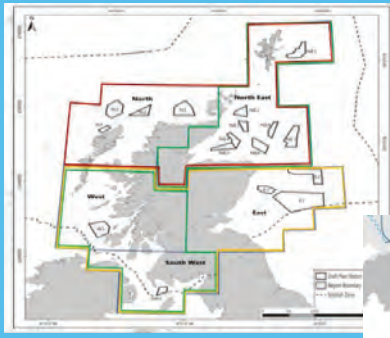
Supervised by: Prof. Beth E Scott, Dr Neda Trifonova, Dr Julie Black & Dr John Hartley

## Wind Energy & Climate change in the UK

40 GW of wind energy by 2030 but room for 100 GW of floating wind in Scotland by 2050

Climate change oceanic drivers by 2100:

17 new Draft Plan Option (DPO) areas potentially suitable for wind energy generation



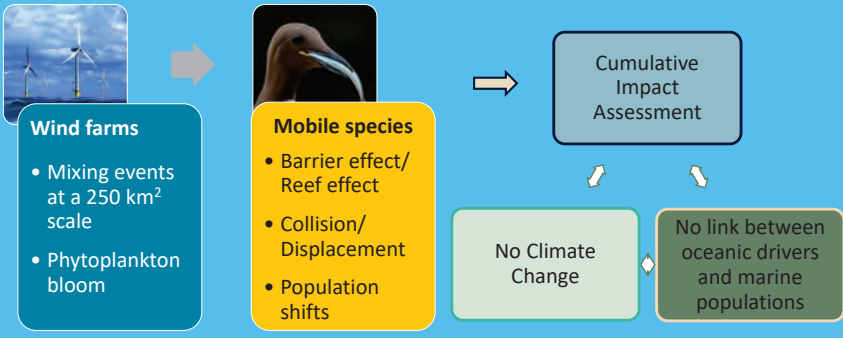
- Warmer sea surface temperatures,
- Longer stratification events
- Decline of Dissolved Oxygen concentration



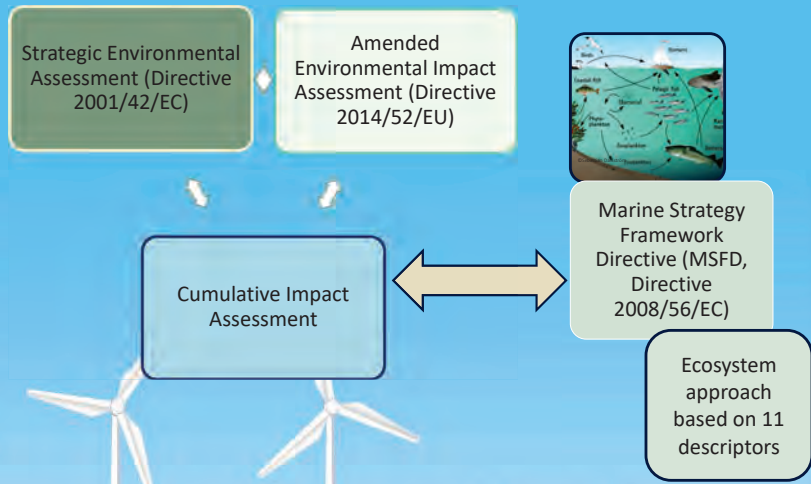
- Shifts of trophic interactions at a scale of 75 km up to 164 km in the North Sea around 2050



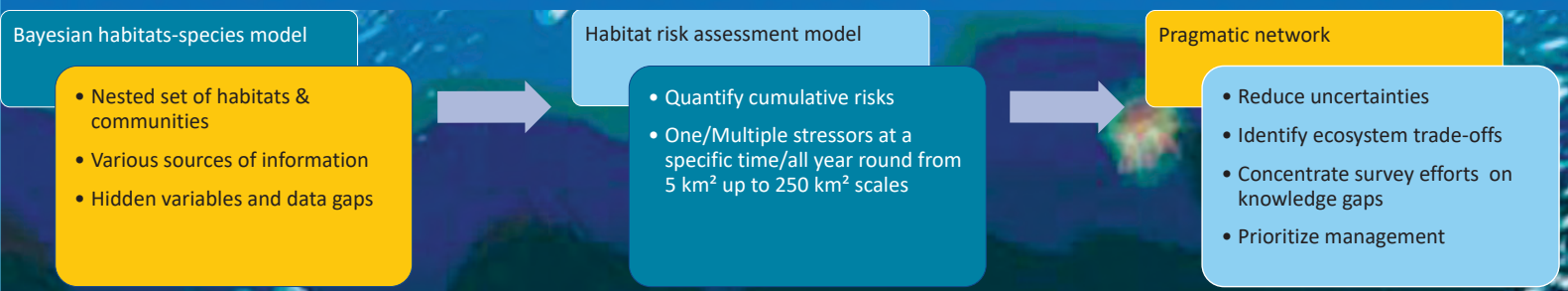
## Gaps in knowledge



## A holistic policy framework for a pragmatic assessment: What should be done ?



## Bayesian habitat risk assessment model for a pragmatic assessment



## Tool Creation: Database & Application



- UK open access collaborative metadata portal
- Compiles 14 000 UK marine datasets from a panel waters commercial sectors, stakeholders and academic
- Create a large scale/high-resolution Wind Energy- Climate Change theme for the cumulative impact assessment



- Linked to Supergen ORE Research landscape Tool and build upon the Bayesian habitat risk assessment model
- Structured by key climate change eco-system drivers & anthropogenic activities (wind energy production goal/shape of array, fisheries)
- Outputs maps of cumulative risk scores to evaluate the broader environmental and natural capital changes

# A new strategic tool to structure Cumulative Impact Assessment (CIA)

Morgane Declerck<sup>1</sup>, Neda Trifonova<sup>2</sup>, Julie Black<sup>3</sup>, John Hartley<sup>4</sup> and Beth Scott<sup>5</sup>

<sup>1</sup> School of Biological Sciences, University of Aberdeen – [m.declerck.19@abdn.ac.uk](mailto:m.declerck.19@abdn.ac.uk)

<sup>2</sup> School of Biological Sciences, University of Aberdeen

<sup>3</sup> Joint Nature Conservation Committee (JNCC)

<sup>4</sup> Hartley Anderson

<sup>5</sup> School of Biological Sciences, University of Aberdeen

To mitigate climate change consequences, the UK government plans to generate 40 GW of offshore wind energy by 2030 with the draft sectoral plan claiming room for up to 100 GW of floating wind just in Scottish waters. The North Sea is a dynamic ecosystem with strong bottom-up/top-down ecological drivers facing rapid climate change impacts. Therefore, to ensure compatibility of such large-scale developments with nature conservation obligations, cumulative effects need to be assessed.

CIA is currently under the authority of both the Strategic Environmental Assessment (SEA) (Directive 2001/42/EC) and the amended Environmental Impact Assessment (Directive 2014/52/EU). The current CIA excludes rapid climate change impacts and thus lacks spatial-temporal appropriate baselines linking ecosystem components (e.g. oceanic drivers) to population dynamics. This leads to uncertain predictions at colonies and populations levels.

This study presents an overview of a framework for CIAs using a holistic and pragmatic ecosystem approach based on a habitat risk Bayesian network in order to identify pressure pathways, keystone components, ecosystem resilience, population-level changes as well as fisheries socio-economic risks. Finally, we will discuss the usefulness of the two components that make up this framework: a database including data sources and an application of standardised shared tools that will pave the way to more transparent and multi-disciplinary collaborations. This framework will provide a multi-dimensional decision-making toolkit that will also lead towards more strategic SEAs as well as providing the ability to embed the CIAs of projects into regional and multinational schemes.

Miad Saberi\*, Harvey J. Burd, Byron W. Byrne  
 Department of Engineering Science, University of Oxford, UK  
 \*Email: miad.saberi @eng.ox.ac.uk

## Introduction

A monopile experiences different lateral environmental loads due to wind and wave. The resulting soil-structure interaction aspects should be considered in the analysis and design of monopiles (see Fig. 1).

Three-dimensional (3D) finite element (FE) analysis has gained extensive popularity in geotechnical practice for simulating the behaviour of laterally loaded monopiles and validating the design process. However, the selection of an efficient constitutive model with a straightforward process for calibrating the input parameters is a challenging issue.

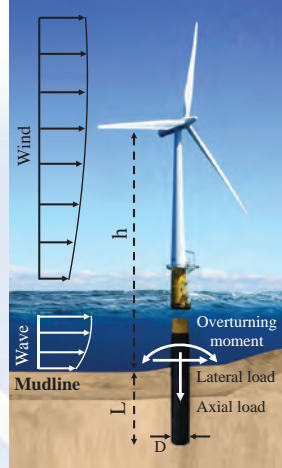


Fig. 1: Monopile under lateral loads

## Objectives

- Developing an efficient and systematic calibration process for the elasto-plastic HSsmall model (Hardening Soil model with small-strain stiffness; Benz 2007) implemented in PLAXIS.
- Predicting the force-displacement relationships for monopiles with different geometries embedded in sand with various densities using 3D FE analysis.
- Validating the analyses by comparing model predictions obtained from the HSsmall model with other approaches.

## Model Calibration & 3D FE Model

The most of the input parameters for HSsmall model (Table 1) can be determined from the soil relative density  $D_r = (e_{max} - e) / (e_{max} - e_{min})$ .

Table 1. HSsmall model parameters

Parameter	Description	Parameter	Description
$\gamma_{sat}$ (kN/m <sup>3</sup> )	Saturated unit weight	$G_0^{ref}$ (MPa)	Reference value of small strain shear modulus
$K_0$	Lateral earth pressure coefficient	$\gamma_{0.7}$	Threshold shear strain at which $G_s = 0.722G_0$
$c'$ (kN/m <sup>2</sup> )	Effective cohesion	$E_{50}^{ref}$ (MPa)	Secant stiffness in standard drained triaxial test
$p^{ref}$ (MPa)	Reference pressure	$E_{oed}^{ref}$ (MPa)	Tangent stiffness for primary oedometer loading
$R_f$	Failure ratio	$E_{ur}^{ref}$ (MPa)	Unloading/reloading stiffness from drained triaxial test
$m$	Power for stress-level dependency of stiffness	$\varphi'$ (deg)	Peak friction angle
$\nu$	Poisson's ratio	$\psi'$ (deg)	Dilation angle

$\gamma_{sat}$  and  $\nu$  are usually the known initial soil parameters.

$c' = 0$  for sand,  $p^{ref} = 100$  kPa, and  $R_f = 0.9$  and  $m = 0.5$  for FE analysis

$$K_0 = 1 - \sin(\varphi') \text{ (Jaky Equation)}$$

$G_0^{ref}$  is determined to give the best fit between the  $G_0$  profiles simulated by the HSsmall model and the Hardin (1978) model (as used in Burd et al. 2020):

$$G_0 = \frac{B p^{ref}}{0.3 + 0.7 e_0^2} \sqrt{\frac{p'}{p^{ref}}} \quad \text{AND} \quad G_0 = G_0^{ref} \left( \frac{c' \cos(\varphi') - \sigma_3' \sin(\varphi')}{c' \cos(\varphi') + p^{ref} \sin(\varphi')} \right)^m$$

Using Brinkgreve (2010):  $\gamma_{0.7} = \left(2 - \frac{D_r}{100}\right) / 10000$  AND  $E_{50}^{ref} = 60000 \frac{D_r}{100}$

$E_{oed}^{ref} = E_{50}^{ref}$  AND  $E_{ur}^{ref} = 3 E_{50}^{ref}$

Relate constant volume friction angle  $\varphi'_{CV}$  and the angle of dilation by (Bolton 1986):  $\varphi' = \varphi'_{CV} + 0.8\psi$

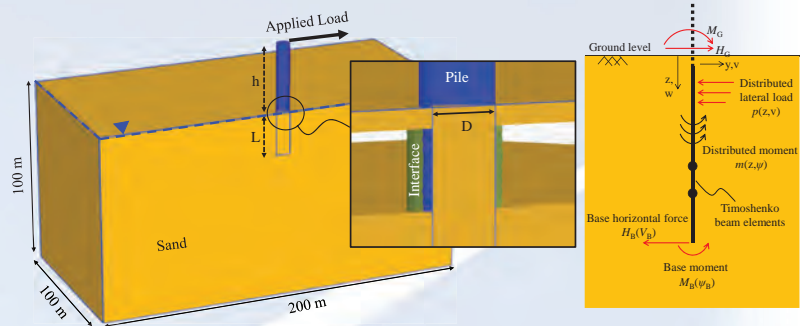


Fig. 2: 3D FE model for laterally loaded monopiles

Fig. 3: 1D FE PISA model (from Burd et al., 2020)

## Numerical Results

The HSsmall model was calibrated for different soil relative densities ( $D_r$ ) and a relationship between  $\varphi'$  and  $D_r$  was developed. The numerical predictions were then compared with 1D FE PISA model using the General Dunkirk Sand Model (Burd et al. 2020) and a 3D FE model with an advanced critical state soil constitutive model in the framework of bounding surface plasticity (Taborda et al. 2014).

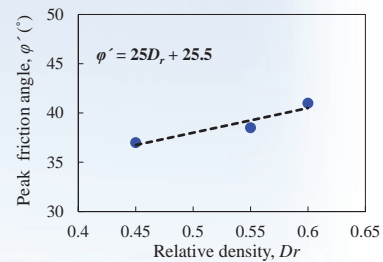


Fig. 4: Predicted  $\varphi'$ - $D_r$  relationship.

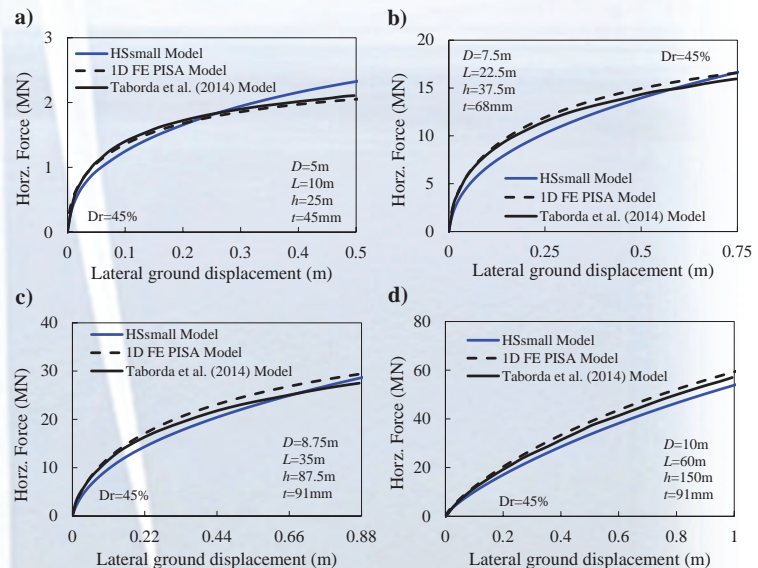


Fig. 5: Numerical predictions of monopiles at ultimate displacement;  $D$ : diameter,  $L$ : embedded length,  $h$ : loading height, and  $t$ : wall thickness.

## References:

- Benz, T. 2007. Small-strain stiffness of soils and its numerical consequences. Stuttgart Universität Stuttgart - Institut für Geotechnik.
- Bolton, M.D. 1986. The strength and dilatancy of sands. Geotechnique, 36(1): 65-78.
- Brinkgreve, R.B.J., Engin, E., and Engin, H.K. 2010. Validation of empirical formulas to derive model parameters for sands. In Numerical Methods in Geotechnical Engineering - Proceedings of the 7th European Conference on Numerical Methods in Geotechnical Engineering, pp. 137-142.
- Burd, H.J., and 12 others. 2020. PISA design model for monopiles for offshore wind turbines: Application to a marine sand. Geotechnique, 70(11): 1048-1066.
- Taborda, D.M.G., Zdravković, L., Kontoe, S., and Potts, D.M. 2014. Computational study on the modification of a bounding surface plasticity model for sands. Computers and Geotechnics, 59: 145-160.

# Three-Dimensional Finite Element Modelling of Laterally Loaded Monopiles in Sand

Miad Saberi\*<sup>1</sup>, Harvey J. Burd<sup>1</sup>, Byron W. Byrne<sup>1</sup>

<sup>1</sup>Department of Engineering Science, University of Oxford, UK

## Abstract

Monopiles are a commonly employed foundation system for offshore wind turbine (OWTs) support structures in shallow coastal waters. Monopiles are single open-ended tubular steel piles with large diameter (in region 10m) which are installed into the seabed. The response of monopile foundations when loaded by wind and wave is governed by the stiffness and strength of the surrounding soil and the monopile-soil interaction. Thus, the design of monopile foundations needs analysis tools to provide reliable predictions for the response of laterally loaded soil-pile interaction mechanisms. The use of three-dimensional (3D) finite element (FE) analysis is widely employed in research and industry for simulating 3D soil-pile interaction problems and validating the design process for monopile foundations. However, the selection of an efficient constitutive model with easily determined input parameters and the ability to provide reliable predictions for nonlinear soil-pile interaction is a challenging subject. In this study, the application of a widely used elasto-plastic constitutive model (HSsmall implemented in PLAXIS) for predicting the behaviour of monopiles embedded in sands is investigated using 3D FE analysis. A simple and systematic process for calibrating the HSsmall constitutive model parameters is developed, and nonlinear lateral load-displacement relationships for monopiles with different geometries in a sand with various soil relative densities are predicted. To validate the approach, the pile response predictions obtained from HSsmall model are then compared with other approaches: 1D FE PISA model and a 3D FE model with an advanced soil constitutive model in the framework of bounding surface plasticity and critical state soil mechanics.

\*Email: miad.saberi @eng.ox.ac.uk

# Origami inspired clam type wave energy converter

Jingyi Yang<sup>1</sup>, Krishnendu Puzhukkil<sup>2</sup>, Xinyu Wang<sup>2</sup>, Alistair Borthwick<sup>2</sup>, Edward Ransley<sup>2</sup>, John Chaplin<sup>3</sup>, Maozhou Meng<sup>2</sup>, Martyn Hann<sup>2</sup>, Robert Rawlinson-Smith<sup>2</sup>, Shanshan Cheng<sup>2</sup>, Siming Zheng<sup>2</sup>, Zhong You<sup>1</sup>, Deborah Greaves<sup>2\*</sup>

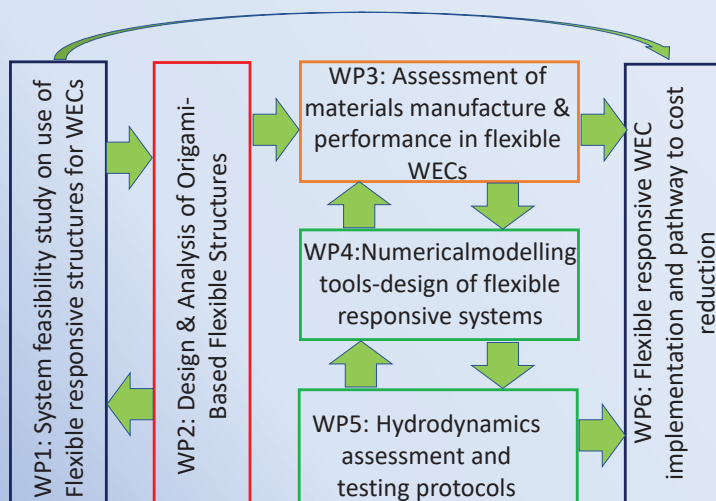
<sup>1</sup> University of Oxford, <sup>2</sup> University of Plymouth, <sup>3</sup> University of Southampton

Contact Email: [krishnendu.puzhukkil@plymouth.ac.uk](mailto:krishnendu.puzhukkil@plymouth.ac.uk), [jingyi.yang@eng.ox.ac.uk](mailto:jingyi.yang@eng.ox.ac.uk), [xinyu.wang-41@plymouth.ac.uk](mailto:xinyu.wang-41@plymouth.ac.uk)

## Design requirements

- Designing a clam-shaped model using **rigid panels** and **flexible membranes** that opens and closes in response to the waves.
- **Not pressurised** but fully enclosed.
- The clam can be **fully closed** and sink to sea-bed (survival mode).
- Potential **PTO**:
  - Dielectric elastomer generator (DEG);
  - Air-turbine generator;
  - Mechanical linear actuators.

## WORK PROGRAMME (August 2021-2024)



## Challenge on material selection

- The material selection for the Origami-inspired design is challenging, especially when these components are designed to survive under **cyclic load and marine environment**.
- Various components require different levels of deformation and response, which need to be made with **different types of elastic materials** and their composites.
- The **connecting components** (e.g., facet to facet joints) can be the most vulnerable, where cyclic folding, shearing and stretching happen.

## Origami-based flexible structures

- Folding a flat sheet according to Fig 1(a) and welding along the red lines, the model in Fig 1(b) can be obtained where yellow cardboards represent rigid side facets and blue membranes are elastic.
- Rigid facets are rotating around the hinges, and elastic membranes are allowed to stretch.
- Predictable, localised tension in the elastic membranes when the structure is in motion.
- Energy loss due to material deformation is minimised.

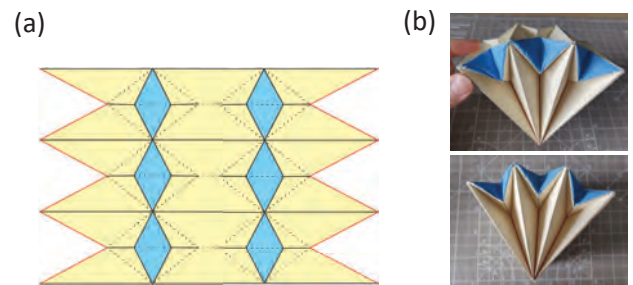


Fig 1. A clam design. (a) The crease pattern, and (b) the prototype.

## Hydrodynamic assessment of flexible membranes

- Preliminary investigation assessing hydro-elastic response of different flexible membranes (Neoprene rubber, Polyurethane, Silicone and Reinforced neoprene rubber) – COAST Lab, University of Plymouth.
- Focused waves & regular waves.
- Laser distance sensor used to measure the response of the membranes.



Fig 2. Photograph of neoprene rubber with four-edge fixed frame

# Origami-inspired clam type wave energy converter

Jingyi Yang<sup>1</sup>, Krishnendu Puzhukkil<sup>2</sup>, Xinyu Wang<sup>2</sup>, Alistair Borthwick<sup>2</sup>, Edward Ransley<sup>2</sup>, John Chaplin<sup>3</sup>, Maozhou Meng<sup>2</sup>, Martyn Hann<sup>2</sup>, Robert Rawlinson-Smith<sup>2</sup>, Shanshan Cheng<sup>2</sup>, Siming Zheng<sup>2</sup>, Zhong You<sup>1</sup>, Deborah Greaves<sup>2\*</sup>

<sup>1</sup>University of Oxford, <sup>2</sup>University of Plymouth, <sup>3</sup>University of Southampton

Contact Email: [krishnendu.puzhukkil@plymouth.ac.uk](mailto:krishnendu.puzhukkil@plymouth.ac.uk), [jingyi.yang@eng.ox.ac.uk](mailto:jingyi.yang@eng.ox.ac.uk), [xinyu.wang-41@plymouth.ac.uk](mailto:xinyu.wang-41@plymouth.ac.uk)

## Abstract

Inspired by origami, an offshore deployable device is designed to effectively capture the wave energy. To function in the sea, the device needs to be waterproof and thus enclosed. As no enclosed rigid body can change its volume without deformation, an enclosed clam-shaped offshore device can be constructed by connecting rigid facets and elastic membranes with rotational hinges. We model the rigid panels to rotate along the hinges without facet deformation and allow stretching on elastic membranes. The strain of the elastic material shall be minimised for a better structural integrity and a minimal energy loss. Satisfying all the design requirements, the best geometric design is obtained through an optimisation process. Based on the optimised geometry, a downscaled prototype was built using rigid plywood to prove that the strain incurred is negligible in response to forces.

The full-scale model shall be partially immersed and is not to be pressurised. Seawater on the top pleats can be drained easily due to the open channel designed on the top pleats. Furthermore, in terms of adverse weather, the clam can turn into its survival model, it will be fully closed and sink to the seabed. The power take-off of the clam design can either be due to volumetric change through a turbine or connecting a dielectric elastomer generator.

Various components require different levels of deformation and response, which need to be made with different types of elastic materials and their composites. The connecting components (e.g., facet to facet joints) can be the most vulnerable, where cyclic folding, shearing, and stretching happen. Therefore, developing a material selection and evaluation scheme is essential for the full-scale mode to understand the life span of the device. The hydro-elastic responses of the flexible membranes are tested in the wave flume facility at the COAST Lab, University of Plymouth. The flexible membrane under investigation includes neoprene rubber, polyurethane, silicone, and reinforced neoprene rubber. The response of the membranes for different focused and regular wave cases were captured using laser distance sensors. The preliminary results on the hydro-elastic response of the membrane can help in designing the full-scale origami inspired clam wave energy converter.